Sign-elevation angle rigidity and its application to bearing-only formation control in agents' local frames

Chinmay Garanayak and Dwaipayan Mukherjee

***Abstract*—In this paper, we propose sign-elevation angle rigidity and design bearing-only control laws in agents' local coordinate frames without any orientation synchronization or estimation algorithms. Moreover, we also establish almost global stability results for formation control, with elevation angle measurements that can be obtained using bearing-only sensors in the agents' local frames. Elevation angle rigidity-based control laws can only guarantee local stability results, and existing results do not address flip, flex, and reflection ambiguities that can arise in elevation angle rigid configurations. Hence, we first establish the theory of sign-elevation angle rigidity to uniquely characterize formation shapes, up to translation and rotation, by employing elevation angle and signed-area constraints for planar frameworks, while for 3-D frameworks, elevation angle constraints along with signed-volume constraints are used. Then, we propose control laws for single integrators and prove almost global stabilization to the desired formation shapes using bearing-only measurements when the desired formation is obtained by triangulated sub-formations for 2-D graphs and tetrahedral sub-formations for 3-D graphs. Control laws for non-holonomic agents are also analyzed. Finally, simulations are provided to validate the obtained results.**

Index terms: bearing-only control, formation ambiguities, coordinate-free control, formation control

I. INTRODUCTION

Recent years have witnessed active research on distributed formation control of multi-agent systems, making it an intriguing area of study [1]–[4]. The primary objective of the formation control problem is to design decentralized control laws for the agents, enabling them to attain a specific geometric shape. An associated problem with formation control is identifying geometric shapes using local constraints, which is addressed through rigidity theory and its extensions.

When using position-based formation control, every agent is restricted to a specific position, and it must be able to detect its exact position for the strategy to work. On the other hand, displacement-based formation control uses displacement constraints between agents to determine the shape of the formation [5]–[7]. This method is related to the consensus protocols in multi-agent systems. In a distance-based formation control strategy, the desired formation is specified by inter-agent distance constraints. Distance rigidity theory deals with how to determine unique formation shapes from distance constraints [1], [8]. The formation control laws that were developed based on distance rigidity required both distance and displacement between the agents [1], [3], [8]–[11]. Using distance and angle constraints, studies such as [12]–[14] have defined formation shapes, leading to the concept of weak-rigidity. The articles [15], [16] introduced the concept of bearing rigidity theory, which can accurately define unique formation shapes up to a translation and scale through the use of bearing constraints for defining the target formation. Additionally, [17] presented the concept of bearing-ratio-of-distance rigidity theory using bearing and ratio-of-distance constraints. However, the control laws for formation control in [16], [17] necessitated inter-agent displacement measurements.

Vision-based applications can benefit from bearing measurements, which have the advantage of utilizing low-cost passive optical sensors such as cameras instead of displacement measurements. Bearing measurements also tend to be less noisy than displacement and distance measurements [18]. Additionally, they require a less complex sensory setup for the agents, resulting in a lower payload on the agents. Hence, bearing-only formation control has received considerable research attention in recent years [4], [18], [19]. The primary objective of bearing-only formation control is to achieve the desired shape of the formation by relying solely on bearing measurements without using inter-agent distance and displacement measurements. In [4], the analysis of bearing-only formation control for single integrators was conducted using bearing rigidity theory, and [19] reported tracking control for single and double integrators, as well as unicycles, with constant velocity leaders. Ref. [20], [21] discussed the implementation of time-varying bearing-only formation control using the concept of persistence of excitation. It is important to note that bearing measurements rely on a specific coordinate system, requiring agents to access a global coordinate system to implement control laws when inter-agent bearing constraints specify the desired formation. However, distance-based formation control laws can be implemented in the agent's local coordinate system, as distance constraints are not dependent on a specific coordinate system. Therefore, to apply bearing-only control laws in agents' local coordinate frame, orientation synchronization [22], [23] or orientation estimation algorithms [24], [25] are typically implemented in conjunction with the formation control law. Also, orientation synchronization or estimation algorithms need relative attitude measurements between the agents, which is difficult to obtain in practice or may require extra relative attitude estimation algorithms from local bearing sensing [26]. Refs. [27], [28] studied bearing-only formation control in agents' local frames based on $SE(2)$ and $SE(3)$ rigidity theories. However, they required extra controllable quantities, which established the relation between agents' local and global frames.

An approach to bearing-only formation control using angle rigidity was suggested for planar agents in [29], [30] to obviate the need for a global coordinate system. This approach

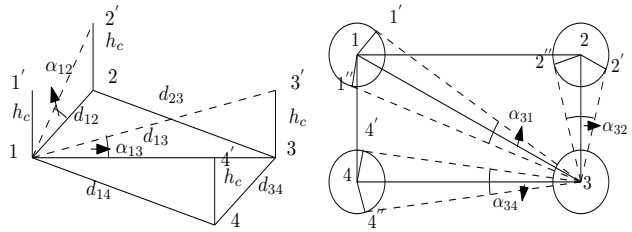
C. Garanayak (chinmayg22@gmail.com) and D. Mukherjee (dm@ee.iitb.ac.in) are with the Department of Electrical Engineering, Indian Institute of Technology Bombay, Mumbai- 400076, India. The work of DM was supported in part by an ISRO funded project bearing code RD/0120-ISROC00-007.

incorporated signed angle constraints in the formation specification and established local exponential convergence to the desired formation shape. In [31], unsigned angle constraints were used to describe the desired formation shape. However, the control law in [31] required inter-agent displacement measurements. In refs. [32], [33] a triangular angle rigidity theory was proposed to describe the desired formation shape using triangular angle constraints. However, the control laws in [33] also required relative displacement between the agents. Ref. [34] discussed the specification of planar agents with circular discs and proposes a bearing-only formation control in a two-dimensional setting. Elevation angle rigidity was addressed [35], which involves attaching a rod to each agent in 2D or a ball to agents in 3D to specify elevation angle constraints and the desired formation was described by these constraints. A gradient-based bearing-only formation control law in the agents' local frames of reference was then proposed, which established local asymptotic stability about the desired formation shape. The constraints on elevation angles were independent of coordinates, so the control laws in [35] did not need information about any global coordinate system. In [36], elevation angle-based control laws were proposed for double integrators and non-holonomic agents. In [37], elevation angle rigidity control laws for single and double integrators were derived in the presence of bounded disturbances. However, it is important to note that setting constraints only on the elevation angles in the formation specification can result in issues such as flip, flex, and reflection ambiguities in the final formation shape, which were not addressed in [35] and only local convergence to the desired formation shape was established in [35]–[37]. In distance-based formation control [38], [39], such ambiguities are also present. In [38], such ambiguities were addressed by using signed area constraints for 2-dimensional scenarios when 3 or 4 agents are employed. Ref. [40] proposed sign-rigidity theory where signed area constraints were used along with distance constraints to address ambiguities in 2-D. Ref. [39] addressed these ambiguities by implementing constraints related to the signed unit area and signed unit volume but only established local convergence results.

In view of the above results, the important contributions of this article are summarized below:
We present sign-elevation angle rigidity to characterize unique formation shapes up to a translation and rotation using elevation angle with signed-area or signed-volume constraints for graphs embedded in Euclidian 2-D or 3-D space, respectively. For checking sign-elevation angle rigidity, the sign-elevation angle rigidity matrix is derived based on the sign-elevation angle rigid motions, and a rank condition on the sign-elevation angle rigidity matrix is provided. Then, we establish almost global convergence to the desired formation shape using only local bearing measurements for both planar and three-dimensional formations when the sign-elevation angle rigid framework is generated by a signed-Henneberg construction. Both single integrators and non-holonomic agents are considered for the control design and stability analysis. In contrast with existing results, our current work has the following salient features:
(i) Compared with bearing-only control laws proposed in [4], [19]–[21], the agents here do not need to know their orientation information with respect to a global frame. Compared with [22]–[24], no extra orientation synchronization or orientation estimation algorithms are needed for the control implementation. Compared with [16], [17], extra degrees of freedom in terms of orientation control are not required.
(ii) Compared with the angle rigidity-based bearing-only control laws in [29], [30], we have used elevation angle constraints in our design. Hence, we do not have any scale ambiguity in the final formation shape. We can obtain a rigid formation in the conventional sense, i.e., the final formation behaves like a rigid body. In contrast, the final formation shape obtained in [29], [30] has translational, rotational, and scale invariance, and due to the scale invariance, the final formation does not behave like a rigid body.
(iii) Compared with [35], [37], where only elevation angle constraints were used, we use signed-area or signed-volume constraints to specify the desired formation shape. Hence, flip, flex, and ordering ambiguity can be eliminated. Also, [29], [30], [34], [35], [37] established only local stability results, whereas we established almost global stability. Hence, agents can converge to the desired shape from arbitrary initial positions. Thus, almost global results are proved for bearing-only formation control in agents' local frame, as a novel contribution of our paper.
(iv) Unlike [33], [41] where inter-agent displacement measurement is required, here only local bearing information is required.
(v) In [42] where a localization approach was adopted to establish global stability, where agents' desired positions were estimated from angle constraints, and then a position based controller was proposed. Hence, in [42] the controller required agents' absolute position measurements for its' implementation, whereas our controller can be implemented directly using vision sensors.
(vi) Although the motivation for using a signed-area comes from [40], the control law in [40] is different from the proposed law here. Hence, the structure of the hessian of the potential function is different here than in [40]. Also, [40] has used inter-agent displacements in the control law, whereas our control law uses bearing-only measurements. Also, we have proved stability for the 3-D case as well, whereas [40] was applicable for only planar graphs, i.e., 2-D agents.

Some preliminary results on sign-elevation angle rigidity were presented in [43]. However, only local stability was reported therein. In this article, we establish almost global stability results, consider non-holonomic agents in the control design, and present a detailed discussion on sign-elevation angle rigidity along with various proofs that were not given in [43].

Notations: $||.||$ is used for 2-norm of a vector, $|.|$ represents modulus operation. For $x = [x_1\ x_2\ x_3]^\top \in \mathbb{R}^3, [x]^\times := \begin{bmatrix} 0 & -x_3 & x_2 \\ x_3 & 0 & -x_1 \\ -x_2 & x_1 & 0 \end{bmatrix} \in \mathbb{R}^{3\times 3}$. Symbols $\hat{i}, \hat{j}, \hat{k}$ represent the orthogonal unit vectors along the x, y, z-axes of the coordinate system, respectively, and $\times$ denotes the cross product. $\langle \cdot, \cdot \rangle$ is the inner product operation. $\text{Diag}\{a_1, \ldots, a_n\} \in \mathbb{R}^{n\times n}$



(a) Elevation angles in 2-D (b) Elevation angles in 3-D

Fig. 1. (a) Elevation angle measurements in 2-D, (b) and in 3-D.

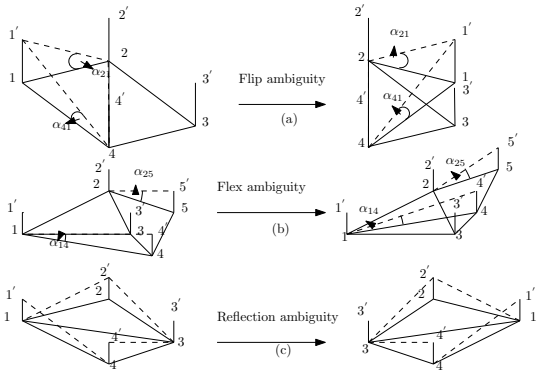


Fig. 2. Formation ambiguities in elevation angle rigid configuration. (a) shows flip ambiguity where elevation angle constraints remain the same when edge $(1,2)$ and $(1,4)$ are flipped over edge $(2,4)$. (b) shows flex ambiguity, and (c) shows reflection ambiguity where there is an ambiguity in the ordering of the agents in configuration.

is a diagonal matrix, where $a_1, \ldots, a_n$ are the diagonal elements. $J = \begin{bmatrix} 0 & 1 \\ -1 & 0 \end{bmatrix}$, and J_1, J_2, $J_3 \in \mathbb{R}^{3\times 3}$ correspond to rotations of $\pi/2$ along the principal axes in $\mathbb{R}^3$.

II. PRELIMINARIES

A. Graph theory

This subsection presents some notions from graph theory [44]. We model the interaction among agents by an undirected graph, $\mathcal{G}(\mathcal{V}, \mathcal{E})$, where $\mathcal{V} = \{1, \ldots, n\}$ is the node-set, and the set of edges is denoted by $\mathcal{E} \subseteq \mathcal{V} \times \mathcal{V}$. The neighbor set of the i-th agent is denoted by $\mathcal{N}_i$, with n_i representing the number of neighbors. The positions of all the agents in $\mathbb{R}^d$ are combined to form a *realization*, denoted by $p := [p_1^\top, \ldots, p_n^\top]^\top \in \mathbb{R}^{nd}$.

B. Agent dynamics

We consider the following systems for control design.

1) Single integrators: Single integrator agents are given by

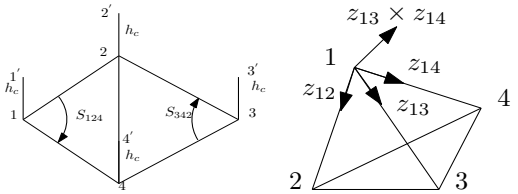
$$\dot{p}_i = u_i \; i \in \mathcal{V}, \tag{1}$$

where $u_i \in \mathbb{R}^d$, $d \in \{2, 3\}$ is the control input.

2) Non-holonomic agents: These are modeled as

$$\dot{p}_i = h_i \bar{v}_i, \; \dot{h}_i = w_i \times h_i \; i \in \mathcal{V}, \tag{2}$$

where $h_i \in \mathbb{R}^d$ is the heading direction of agent i, $\bar{v}_i \in \mathbb{R}$ is the speed along the heading direction , $w_i \in \mathbb{R}^d$ is the angular velocity. The control inputs are $\bar{v}_i$ and w_i.



(a) signed-area (b) signed-volume

Fig. 3. (a) $S_{124} = h_c^{-2}||z_{12}||||z_{14}||\sin(\theta^1_{24})$, and $S_{342} = h_c^{-2}||z_{34}||||z_{32}||\sin(\theta^2_{43})$, (b) $V_{1234} = r_c^{-3} z_{12}^\top (z_{13} \times z_{14})$.

C. Elevation angle rigidity

These are defined in [35]. The elevation angle is obtained by attaching a rod of height h_c with each agent for the planar case, i.e., for 2-D, and for 3-D, each agent is attached with a rod of height r_c. Let $z_{ij} := p_j - p_i, d_{ij} := ||z_{ij}||$ and $b_{ij} := \frac{z_{ij}}{||z_{ij}||} = \frac{z_{ij}}{d_{ij}}$ is the relative displacement, distance, and the bearing vector between agents i and j, respectively. For the 2-D case, the final position of the rod attached with agent i is $p_i^{'} := [p_i^\top \; 0]^\top + [0 \; 0 \; h_c]^\top$. Now, the elevation angle measured by agent i towards agent j is given by $\angle j^{'} ij = \alpha_{ij} := \arccos(\bar{b}_{ij}^\top b_{ij}^{'}) = \text{arccot}(\frac{d_{ij}}{h_c}) \in (0, \frac{\pi}{2})$, where $\bar{b}_{ij} := [b_{ij}^\top \; 0]^\top$. For 3-D case the elevation angle is defined as $\angle j^{'} ij^{''} = \alpha_{ij} := \arccos(b_{ij^{'}}^\top b_{ij^{''}}) = 2\angle j^{'} ij = 2\text{arcsin}(\frac{r_c}{d_{ij}}) \in (0, \frac{\pi}{3})$. The points $j^{'}$ and $j^{''}$ are obtained by drawing tangents from agent i to the ball attached with agent j such that $i, j, j^{'}, j^{''}$ lies on the same plane. Fig. 1 shows elevation α_{12} and α_{13} for 2-D case, and $\alpha_{31}, \alpha_{32}, \alpha_{34}$ for 3-D case, respectively.The elevation angle function is defined as $E(p) : \mathbb{R}^{dn} \to \mathbb{R}^{m_e}$, $E(p) := [f_1, \ldots, f_{m_e}]^\top$, where $f_k := \cot(\alpha_k) = \frac{\cos(\alpha_{ij})}{\sin(\alpha_{ij})} = \frac{d_{ij}}{h_c}$, $k \in \mathcal{E}$, $|\mathcal{E}| = m_e$, and $f_k \in (0, \infty)$ for 2-D, and $f_k := \text{cosec}(\frac{\alpha_k}{2}) = \text{cosec}(\frac{\alpha_{ij}}{2}) = \frac{d_{ij}}{r_c}$, $k := (i, j) \in \mathcal{E}$, $|\mathcal{E}| = m_e$, and $f_k \in (2, \infty)$ for 3-D. When elevation angle constraints define the desired formation,

$$f_k = f_k^*, \; k := (i, j) \in \mathcal{E} \implies E = E^*. \tag{3}$$

Note that a double subscript, such as f_{ij}, will be used to describe neighboring nodes/agents involved. A single subscript, like f_k, can also be used where k is the edge index. The derivative of the elevation angle constraints yields

$$\frac{df_{ij}}{dt} = \begin{cases} h_c^{-1} b_{ij}^\top (v_j - v_i) \text{ (for } 2-\text{D)} \\ r_c^{-1} b_{ij}^\top (v_j - v_i) \text{ (for } 3-\text{D)}. \end{cases} \tag{4}$$

The elevation angle rigidity matrix is defined by: $R_e := \frac{\partial E}{\partial p} \in \mathbb{R}^{m_e \times dn}$, where $d \in \{2, 3\}$ is the dimension of ambient space.

III. MAIN RESULTS

In this section, we first present sign-elevation angle rigidity theory. Then, we design suitable control laws for single integrators and non-holonomic agents and prove stability with the proposed control laws.

A. Signed-area and Signed-volume constraints

In [35], elevation angle constraints are used to specify the desired formation. Specifically, the vector containing the desired elevation angle constraints was denoted as E^*, and it was set to be equal to the actual elevation angle E. The elevation angle constraints remained constant despite flip, flex, or reflection ambiguities, as described in Fig. 2. Ref. [43, Section III A, B] provides further details on these ambiguities. Motivated by [40], we incorporate signed area constraints for 2-D and signed volume constraints for 3-D to address these ambiguities. The signed area constraint is given by

$$\begin{aligned} S_{ijk} &= h_c^{-2} z_{ij}^\top J z_{ik} = \text{constant} = S^*_{ijk} \qquad (5)\\ \implies S_{ijk} &= f_{ij} f_{ik} \sin(\theta^i_{jk}) = S^*_{ijk}, (i,j),(i,k) \in \mathcal{E}, \end{aligned}$$

where $\sin(\theta^i_{jk}) = -\sin(\pi + \theta^i_{jk}),\ \forall\ \theta^i_{jk} \in [0,\pi]$, where at vertex i, the angle formed by edges (i,j) and (i,k) in the direction from (i,j) to (i,k) is represented by $\overset{i}{jk}$. Fig. 3(a) shows two area constraints $S_{124} := f_{12} f_{14} \sin(\theta^1_{24})$ and $S_{342} := f_{34} f_{32} \sin(\theta^3_{42})$, where θ^1_{24} is the angle from z_{12} to z_{14} in the clockwise sense, and θ^3_{42} is from z_{34} to z_{32} in the anticlockwise sense. Hence, for ambiguities like flip, flex, and reflection (ordering), the sign of the area changes. Similarly, for 3-D, the signed-volume constraints are used, which are given by

$$\begin{aligned} V_{ijkl} &= r_c^{-3} z_{ij}^\top (z_{ik} \times z_{il}) = V^*_{ijkl}\ (i,j),(i,k),(i,l) \in \mathcal{E},\\ \implies V_{ijkl} &= f_{ij} f_{ik} f_{il} b_{ij}^\top (b_{ik} \times b_{il}) = V^*_{ijkl}. \qquad (6) \end{aligned}$$

Here, r_c is the radius of the ball attached to each agent. Fig 3(b) illustrates a signed-volume constraint $V_{1234} = r_c^{-3} z_{12}^\top (z_{13} \times z_{14}) = f_{12} f_{13} f_{14} b_{12}^\top (b_{13} \times b_{14})$, and the directions of different vectors involved in it are shown. We may observe that for ambiguous configurations, the magnitude of the area or volume remains the same, but its sign (positive or negative) will change. Hence, the nomenclature signed-area or signed-volume is used. The multiplication of h_c^{-2} in (3), and r_c^{-3} in (6) will help in avoiding the knowledge of h_c and r_c by the agents in the control law. To specify the desired formation, a set of elevation angle constraints is used along with an additional set of signed-area or signed-volume constraints that are appropriately selected for 2-D and 3-D, respectively. All the signed-area constraints are stacked to obtain $S := [S_1, \ldots, S_{m_s}]^\top \in \mathbb{R}^{m_s}$, and all the signed-volume constraints are stacked in $V = [V_1, \ldots, V_{m_v}]^\top \in \mathbb{R}^{m_v}$. The subscripts for the area/volume constraints may be expressed as a single variable or as three/four variables (when the nodes involved are specified).

Definition 1. *(Framework) Define an area index set for 2-D as $\mathcal{A} = \{(i,j,k) \in \mathcal{V}^3 | S_{ijk} \in S\}$ to characterize the subtended angle $\theta^i_{jk} \in [0,\pi]$ or equivalently the area formed by the edges (i,j) and (i,k). Similarly, in 3-D the volume index set is defined by $\mathcal{A} = \{(i,j,k,l) \in \mathcal{V}^4 | V_{ijkl} \in V\}$. Now, a* framework *associated with $\mathcal{G}$ and p is denoted as $\mathcal{F}(\mathcal{G}, p, \mathcal{A})$, where p represents a realization.*

Remark 1. *The ordering of the edges matters while defining the angle set, as it is generated by the edges to characterize the signed-area and signed-volume. Hence, $(i,j,k) \in \mathcal{A} \nRightarrow (j,k,i) \in \mathcal{A}$, for 2-D. Similarly, $(i,j,k,l) \in \mathcal{A} \nRightarrow (j,k,l,i) \in \mathcal{A}$, for 3-D.*

B. Sign-elevation angle rigidity in 2-D

Now, we develop the notion of sign-elevation angle rigidity in 2-D to characterize geometric shapes of a graph embedded in a plane from elevation angle and signed-area constraints.

Definition 2. *(Equivalence of formations) Two frameworks, $\mathcal{F}_1(\mathcal{G}, p, \mathcal{A})$ and $\mathcal{F}_2(\mathcal{G}, q, \mathcal{A})$, over the same graph $\mathcal{G}(\mathcal{V}, \mathcal{E})$ and set $\mathcal{A}$, are* equivalent *in 2-D if*

$$\begin{aligned} \alpha_{ij}(p_i, p_j) &= \alpha_{ij}(q_i, q_j)\ \forall (i,j) \in \mathcal{E},\\ S_{ijk}(p_i, p_j, p_k) &= S_{ijk}(q_i, q_j, q_k)\ \forall (i,j,k) \in \mathcal{A}. \end{aligned}$$

Definition 3. *(Congruence of formations) Two frameworks $\mathcal{F}_1(\mathcal{G}, p, \mathcal{A})$ and $\mathcal{F}_2(\mathcal{G}, q, \mathcal{A})$, over the same graph $\mathcal{G}(\mathcal{V}, \mathcal{E})$ and set $\mathcal{A}$, are* congruent *in 2-D if*

$$\begin{aligned} \alpha_{ij}(p_i, p_j) &= \alpha_{ij}(q_i, q_j)\ \ i,j \in \mathcal{V},\\ S_{ijk}(p_i, p_j, p_k) &= S_{ijk}(q_i, q_j, q_k)\ \ i,j,k \in \mathcal{V}. \end{aligned}$$

Definition 4. *(Sign-elevation angle rigidity) A framework $\mathcal{F}(\mathcal{G}, p, \mathcal{A})$ is sign-elevation angle rigid if there exists an $\epsilon > 0$ such that, all equivalent frameworks $\mathcal{F}'(\mathcal{G}, q, \mathcal{A})$ in 2-D satisfying $||p - q|| < \epsilon$ are congruent to it.*

Definition 5. *(Global sign-elevation angle rigidity) A framework, $\mathcal{F}(\mathcal{G}, p, \mathcal{A})$, is globally sign-elevation angle rigid if any other framework $\mathcal{F}'(\mathcal{G}, q, \mathcal{A})$ that is equivalent to $\mathcal{F}(\mathcal{G}, p, \mathcal{A})$, is congruent to it.*

Next, we introduce the notion of infinitesimal sign-elevation angle rigidity. For this, we first define the following sign-elevation angle rigidity function: $F^s_e : \mathcal{X} \to \mathbb{R}^{(m_e + m_s)}$, where $\mathcal{X} \subset \mathbb{R}^{2n}$:

$$F^s_e(p) := [f_1 \ldots, f_{m_e}, S_1, \ldots, S_{m_s}]^\top, \qquad (7)$$

where $E = [f_1, \ldots, f_{m_e}]^\top \in \mathbb{R}^{m_e}$, and $S = [S_1, \ldots, S_{m_s}]^\top \in \mathbb{R}^{m_s}$ are the vectors containing the elevation angle constraints, and signed-area constraints, respectively. The number of elevation angle constraints and signed area constraints is m_e and m_s, respectively. Now, we define the infinitesimal sign-elevation angle rigid motions of a framework, which are motions of the framework $\mathcal{F}$ on a differentiable path, $\varrho(t)$, such that the sign-elevation angle rigidity function, i.e., F^s_e, remains constant, i.e., $\dot{F}^s_e \equiv 0$. We say that infinitesimal motions of the entire framework ($\dot{p}$) are *trivial* if they correspond to only translations and rotations of the desired formation shape. Equivalently, the trivial motions of the framework are given by

$$p_i(t) = R(t) p_i(t_0) + T(t),\ i \in \mathcal{V}, t > 0,$$

where $R(t) \in \mathbb{R}^{2\times 2}$ and $T(t) \in \mathbb{R}^2$ represent rotation and translation motions in $\mathbb{R}^2$. The infinitesimal sign-elevation angle rigidity is introduced to characterize all the trivial motions of the framework.

Remark 2. *From Definition 4, it is clear that a framework, $\mathcal{F}(\mathcal{G}, p, \mathcal{A})$, is sign-elevation angle rigid if there exists a*

neighborhood, $\mathcal{U}_p$, around p such that $(F_e^s)^{-1}(F_e^s(p)) \cap \mathcal{U}_p = (F^s_{\frac{n(n-1)}{2}})^{-1}(F^s_{\frac{n(n-1)}{2}}(p)) \cap \mathcal{U}_p$, where $F^s_{\frac{n(n-1)}{2}}$ is the sign-elevation angle rigidity function for a complete graph.

Definition 6. *(Infinitesimal sign-elevation angle rigidity) We say a framework is infinitesimal sign-elevation angle rigid if all of its infinitesimal motions are trivial.*

Next, we introduce the sign-elevation angle rigidity matrix, R_e^s, which is defined as the Jacobian of the elevation angle-sign rigidity function, i.e.,

$$R_e^s := \frac{\partial F_e^s}{\partial p} = \begin{bmatrix} \frac{\partial E}{\partial p} \\ \\ \frac{\partial S}{\partial p} \end{bmatrix} = \begin{bmatrix} R_e \\ \\ R_s \end{bmatrix} \in \mathbb{R}^{(m_e+m_s)\times 2n}. \quad (8)$$

Taking the derivative of signed area constraints in (5), we get

$$\begin{aligned} &\frac{dS_{ijk}}{dt} = h_c^{-2} z_{ij}^\top J(v_k - v_i) + h_c^{-2} z_{ik}^\top J^\top (v_j - v_i) = 0 \\ &\Rightarrow h_c^{-1} \left(\frac{||z_{ij}||}{h_c} b_{ij}^\top J(v_k - v_i) + \frac{||z_{ik}||}{h_c} b_{ik}^\top J^\top (v_j - v_i) \right) = 0 \\ &\Rightarrow h_c^{-1} f_{ij} b_{ij}^\top J(v_k - v_i) + h_c^{-1} f_{ik} b_{ik}^\top J^\top (v_j - v_i) = 0, \quad (9) \end{aligned}$$

where v_i, v_j, v_k are infinitesimal motions (i.e. velocities) of agents i, j, k, respectively. We combine (4) and (9) to get

$$\dot{F}_e^s = \frac{\partial F_e^s(p)}{\partial p} \dot{p} = \begin{bmatrix} \frac{\partial E}{\partial p} \\ \\ \frac{\partial S}{\partial p} \end{bmatrix} \dot{p} = 0. \quad (10)$$

The following Lemma and the subsequent theorem provide a way of checking the infinitesimal rigidity of a framework.

Lemma 1. *For the sign-elevation angle rigidity matrix, we have $L_p := span\{1_n \otimes I_2, (I_n \otimes J)p\} \subseteq Null(R_e^s)$, and $Rank(R_e^s) \leq 2n-3$.*

Proof. From [35, Lemma 1] it is known that $\text{span}\{1_n \otimes I_2, (I_n \otimes J)p\} \subseteq \text{Null}(R_e)$. As $R_e^s = \begin{bmatrix} R_e \\ R_s \end{bmatrix}$, we need to show that $\text{span}\{1_n \otimes I_2, (I_n \otimes J)p\} \subseteq \text{Null}(R_s)$. Define the new edge set as $\mathcal{E}' := \mathcal{E} \cup \mathcal{E}_s$, where $\mathcal{E}_s = \{(i,j),(i,k) | (i,j,k) \in \mathcal{A}\}$. Let, $m_t = |\mathcal{E}'|$. With the new edge set the induced graph is denoted by $\mathcal{G}' = (\mathcal{V}, \mathcal{E}')$. We have $R_s = \frac{\partial S}{\partial p} = \frac{\partial S}{\partial z'} \frac{\partial z'}{\partial p} = \frac{\partial S}{\partial z'} \bar{H}'$, where $z' = [z_1^\top, \ldots, z_{m_t}^\top]^\top$, $z_k \in \mathcal{E}'$, and $\bar{H}' = (H' \otimes I_2)$, with H' being the incidence matrix of graph $\mathcal{G}'$. Now, $\text{span}\{1_n \otimes I_2\} \subseteq \text{Null}(\bar{H}' \otimes I_2)$, implies $\text{span}\{1_n \otimes I_2\} \subseteq R_e^s$. We consider the l-th element in S, i.e., $S_l = h_c^{-2} z_p^\top J z_q$, where $l \in \{1, \ldots, m_s\}$, and $p, q \in \{1, \ldots, m_t\}$. Now, $\frac{\partial S_l}{\partial p}(I_n \otimes J)p = \frac{\partial S_l}{\partial z'} \frac{\partial z'}{\partial p}(I_n \otimes J)p = \frac{\partial S_l}{\partial z'} \bar{H}'(I_n \otimes J)p = h_c^{-2} \frac{\partial z_p^\top J z_q}{\partial z'} \bar{H}'(I_n \otimes J)p$. Also, $\bar{H}'(I_n \otimes J)p = (H' \otimes I_3)(I_n \otimes J)p = (H' \otimes J) = (I_{m_t} \otimes J)(H' \otimes I_2)p = (I_{m_t} \otimes J)z' = [(Jz_1)^\top, \ldots, (Jz_{m_t})^\top]^\top$. Hence, $\frac{\partial z_p^\top J z_q}{\partial z'} \bar{H}'(I_n \otimes J)p = \frac{\partial z_p^\top J z_q}{\partial z'} [(Jz_1)^\top, \ldots, (Jz_{m_t})^\top]^\top = \frac{\partial z_p^\top J z_q}{\partial z_p} J z_p + \frac{\partial z_p^\top J z_q}{\partial z_q} J z_q = \big((z_p)^\top z_q - ((z_q)^\top z_p)\big) = 0$. Thus, for all $l \in \{1, \ldots, m_s\}$, we have $\frac{\partial S_l}{\partial p}(I_n \otimes J)p = R_s(I_n \otimes J)p = 0$, implying $\text{span}\{(I_n \otimes J)p\} \subseteq \text{Null}(R_s(p))$. Hence, $\text{span}\{1_n \otimes I_2, (I_n \otimes J)p\} \subseteq \text{Null}(R_e^s)$. □

Theorem 1. *In 2-D, a framework $(\mathcal{G}, p, \mathcal{A})$ is infinitesimal sign-elevation angle rigid if and only if rank(R_e^s)= $2n-3$.*

Proof. From Lemma 1 it follows that rank of R_e^s is less than or equal to $2n-3$, and $\text{span}\{1_n \otimes I_2, (I_n \otimes J)p\} \subseteq \text{Null}(R_e^s)$. Observe that $1_n \otimes I_2$ corresponds to rigid body translation in 2-D (i.e., translation in the direction of $\hat{i}$ and $\hat{j}$ in a plane), and $(I_n \otimes J)p$ corresponds to rigid body rotation in 2-D, which are the trivial infinitesimal rigid body motions. Hence, we have $\text{rank}(R_e^s) = 2n-3$ if and only if these trivial motions satisfy eqn. (10). Thus, by Definition 6, the framework $(\mathcal{G}, p, \mathcal{A})$ is infinitesimal sign-elevation angle rigid. □

Theorem 2. *A framework $\mathcal{F}(\mathcal{G}, p, \mathcal{A})$ is sign-elevation angle rigid if it is infinitesimal sign-elevation angle rigid.*

Proof. We know from Definition 6 that if the framework $\mathcal{F}(\mathcal{G}, p, \mathcal{A})$ is infinitesimal signed-elevation angle rigid, all of the continuous infinitesimal motions of $p(t)$ of the framework are trivial. In other words, these motions only correspond to rigid body translations and rotations. Now, let us consider another framework $\mathcal{F}'(\mathcal{G}, p', \mathcal{A})$ which is equivalent to $\mathcal{F}(\mathcal{G}, p, \mathcal{A})$, and $||p - p'|| < \epsilon$. In this case, the continuous motions that take p to p' while maintaining $F_e^s = (F_e^s)^*$ are also trivial motions, meaning they only involve translation and rotation of the framework. Therefore, the relation in Definition 3 is satisfied, and we can conclude that $\mathcal{F}'(\mathcal{G}, p', \mathcal{A})$ is congruent to $\mathcal{F}(\mathcal{G}, p, \mathcal{A})$. □

Definition 7. *[40, Definition 2.2](Strong Distance rigidity) A distance rigid framework $\mathcal{F}(\mathcal{G}, p)$ in 2-D is called strongly distance rigid if we have $(p_i - p_j)$ and $(p_i - p_k)$ are independent for all $(i,j),(i,k) \in \mathcal{E}$.*

Proposition 1. *If a framework $\mathcal{F}(\mathcal{G}, p)$ is strongly distance rigid in $\mathbb{R}^2$, then the signed framework $\mathcal{F}_1(\mathcal{G}_1, p, \mathcal{A})$, where $\mathcal{G}_1 = \mathcal{G}$ (i.e., sensing topology for distances in distance rigid graph $\mathcal{G}$ is the same as the elevation angle constraints in $\mathcal{G}_1$), is infinitesimally sign-elevation angle rigid in $\mathbb{R}^2$.*

Proof. Consider the signed framework $\mathcal{F}_1(\mathcal{G}_1, p, \mathcal{A})$ with its elevation angle constraints replaced by distance constraints. As we have $\mathcal{F}(\mathcal{G}, p)$ strongly distance rigid in 2-D, using [10, Proposition 1] $\mathcal{F}(\mathcal{G}, p)$ is infinitesimal distance rigid. Now, a framework is elevation angle rigid if and only if it is distance rigid [35, Proposition 2]. Hence, the framework with elevation angle constraints $\mathcal{F}(\mathcal{G}_1, p)$ is elevation angle rigid. So, there exists a non zero $(2n-3) \times (2n-3)$ minor of R_e [35]. Now, from the definition of sign-elevation angle rigidity matrix $R_e^s = \begin{bmatrix} R_e \\ R_s \end{bmatrix}$ there exists a $2n-3 \times 2n-3$ non zero minor for R_e^s. Then, the proof follows from Theorem 3. □

1) sign-elevation-Henneberg construction in 2-D: (Constructing globally sign-elevation angle rigid frameworks:) To generate rigid frameworks with global sign elevation angle, we adopt a method named sign-elevation-Henneberg construction. The steps of this method are as follows. First, we assume the initial framework has $|\mathcal{V}| = 3, |\mathcal{E}| = 3$, and $\mathcal{A} = 1$, i.e., we have 3 elevation angle and 1 signed-area constraints. For a given globally sign elevation angle

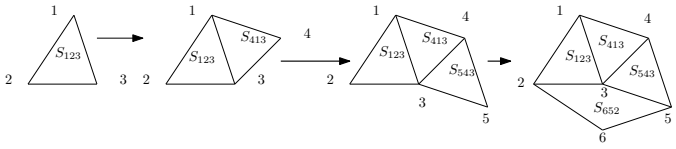


Fig. 4. Example of sign-elevation-Henneberg construction method for generating globally sign-elevation angle rigid frameworks in 2-D.

rigid framework $\mathcal{F}(\mathcal{G}, p, \mathcal{A})$, an agent v is added to it such that it has two more elevation angle constraints and one signed-area constraint. Now the new framework $\bar{\mathcal{F}}(\bar{\mathcal{G}}, \bar{p}, \bar{\mathcal{A}})$ consists of triangular frameworks and $\bar{\mathcal{G}} = (\bar{\mathcal{V}}, \bar{\mathcal{E}}), \bar{\mathcal{V}} = \mathcal{V} \cup \{v\}, \bar{\mathcal{E}} = \mathcal{E} \cup \{(i,v),(j,v)\}, \bar{\mathcal{A}} = \mathcal{A} \cup \{(\bar{i},\bar{j},\bar{k})\}$, and $p = [p^\top \ p_v^\top]^\top \in \mathbb{R}^{2(n+1)}$, where $i,j \in \mathcal{V}, \bar{i},\bar{j},\bar{k} \in \{i,j,v\}$ and $\bar{i} \neq \bar{j} \neq \bar{k}$, also i,j,v should not be co-linear. Fig. 4 demonstrates the steps used in this method.

Proposition 2. *An infinitesimally sign-elevation angle rigid framework $\mathcal{F}(\mathcal{G}, p, \mathcal{A})$ is globally sign elevation angle rigid if it results from a sign-elevation-Henneberg construction.*

Proof. As the framework, $\mathcal{F}(\mathcal{G}, p, \mathcal{A})$, is infinitesimally sign-elevation angle rigid, from Theorem 1 we have $\text{rank}(R_e^s) = 2n-3$. Hence, from Lemma 1, R_e^s is of maximal row rank, and using [8, Proposition 2] there exists a neighbourhood $\mathcal{U}_p$ such that $(F_e^s)^{-1}(F_e^s(p)) \cap \mathcal{U}_p$ is a 3-dimensional smooth manifold which corresponds to 2-D rigid transformations. Further, from Definition 4, it follows that $\mathcal{F}(\mathcal{G}, p, \mathcal{A})$ is sign-elevation angle rigid. In addition, using signed Henneberg construction, we can uniquely determine the position of each agent, as the position of each agent in a sequence is uniquely determined by 2 elevation angle and 1 area constraints. Hence, from Definition 5, we conclude that $\mathcal{F}(\mathcal{G}, p, \mathcal{A})$ is globally sign-elevation angle rigid. □

C. Sign-elevation angle rigidity in 3-D

In this subsection, sign-elevation angle rigidity is developed in 3-D. We have for $x, y \in \mathbb{R}^3$, $x \times y = [x]^\times y$.

Definition 8. *(Equivalence of formations) Two frameworks in 3-D, $\mathcal{F}_1(\mathcal{G}, p, \mathcal{A})$ and $\mathcal{F}_2(\mathcal{G}, q, \mathcal{A})$, over the same graph $\mathcal{G}(\mathcal{V}, \mathcal{E})$, and angle set $\mathcal{A}$, are equivalent if*

$$\alpha_{ij}(p_i, p_j) = \alpha_{ij}(q_i, q_j) \ \forall (i,j) \in \mathcal{E},$$
$$V_{ijkl}(p_i, p_j, p_k, p_l) = V_{ijkl}(q_i, q_j, q_k, q_l) \forall (i,j,k,l) \in \mathcal{A}.$$

Definition 9. *(Congruence of formations) Two frameworks in 3-D, $\mathcal{F}_1(\mathcal{G}, p, \mathcal{A})$ and $\mathcal{F}_2(\mathcal{G}, q, \mathcal{A})$, over the same graph $\mathcal{G}(\mathcal{V}, \mathcal{E})$, and angle set $\mathcal{A}$, are congruent if*

$$\alpha_{ij}(p_i, p_j) = \alpha_{ij}(q_i, q_j) \ i,j \in \mathcal{V}$$
$$V_{ijkl}(p_i, p_j, p_k, p_l) = V_{ijkl}(q_i, q_j, q_k, q_l) \ i,j,k,l \in \mathcal{V}.$$

Definition 10. *(Sign-elevation angle rigidity) A framework $\mathcal{F}(\mathcal{G}, p, \mathcal{A})$ is sign-elevation angle rigid if there exists an $\epsilon > 0$ such that, all frameworks $\mathcal{F}'(\mathcal{G}, q, \mathcal{A})$ in 3-D satisfying $||p - q|| < \epsilon$ are congruent to it.*

Let m_e represent the number of elevation angle constraints and m_v represent the number of signed volume constraints. We introduce the following elevation angle-sign rigidity function $F_e^v : \mathcal{X} \to \mathbb{R}^{(m_e+m_v)}$, where $\mathcal{X} \subset \mathbb{R}^{3n}$.

$$F_e^v(p) := [f_1 \ldots, f_{m_e}, V_1, \ldots, V_{m_v}]^\top. \tag{11}$$

Combining (3) and (6), we get $\dot{F}_e^v = \frac{\partial F_e^v(p)}{\partial p}\dot{p} = \begin{bmatrix} \frac{\partial E}{\partial p} \\ \\ \frac{\partial V}{\partial p} \end{bmatrix} \dot{p} = 0$, where $E = [f_1, \ldots, f_{m_e}]^\top \in \mathbb{R}^{m_e}$ and $V = [V_1, \ldots, V_{m_v}]^\top \in \mathbb{R}^{m_v}$ are the vectors that comprise the elevation angle constraints and signed-volume constraints, respectively. The sign-elevation angle rigidity matrix, denoted as R_e^v, is defined as the Jacobian of the elevation angle-sign rigidity function, i.e.,

$$R_e^v := \frac{\partial F_e^v}{\partial p} = \begin{bmatrix} \frac{\partial E}{\partial p} \\ \\ \frac{\partial V}{\partial p} \end{bmatrix} = \begin{bmatrix} R_e \\ \\ R_v \end{bmatrix} \in \mathbb{R}^{(m_e+m_v)\times 3n}.$$

Taking the derivative of the volume constraint (6) gives,

$$\begin{aligned} \frac{dV_{ijkl}}{dt} &= r_c^{-3} z_{ij}^\top (z_{ik} \times (v_l - v_i)) - r_c^{-3} z_{ij}^\top (z_{il} \times (v_k - v_i)) \\ &+ (z_{ik} \times z_{il})^\top (v_j - v_i) \\ &= r_c^{-1}(f_{ij} f_{ik} b_{ij}^\top ([b_{ik}]^\times (v_l - v_i) - f_{ij} f_{il} b_{ij}^\top ([[b_{il}]^\times (v_k - v_i)) \\ &- f_{ik} f_{il} b_{il}^\top ([b_{ik}]^\times (v_j - v_i)), \end{aligned} \tag{12}$$

where v_i, v_j, v_k, v_l are velocities of agents i,j,k,l.

Lemma 2. *For the sign-elevation angle rigidity matrix (R_e^v), we have $L_p := \text{span}\{1_n \otimes I_3, (I_n \otimes J_1)p, (I_n \otimes J_2)p, (I_n \otimes J_3)p\} \subseteq \text{Null}(R_e^v)$, and $\text{Rank}(R_e^v) \leq 3n - 6$.*

Proof. The proof is similar to that of Lemma 1. □

Theorem 3. *In 3-D, a framework $(\mathcal{G}, p, \mathcal{A})$ is infinitesimal sign-elevation angle rigid if and only if rank(R_e^s)$= 3n - 6$.*

Proof. From Lemma 2 it is clear that rank of R_e^v is less than or equal to $3n-6$, and span$\{1_n \otimes I_3, (I_n \otimes J_1)p, (I_n \otimes J_2)p, (I_n \otimes J_3)p\} \subseteq$ Null(R_v^e). Observe that $1_n \otimes I_3$ corresponds to rigid body translations in 3-D (i.e. translations along $\hat{i}$, $\hat{j}$, and $\hat{k}$), and $(I_n \otimes J_\beta)p$, $\beta = 1,2,3$ correspond to rigid body rotations, which are the trivial infinitesimal rigid body motions in 3-D. Hence, clearly rank$(R_e^v) = 3n - 6$ if and only if these trivial motions satisfy eqn. (10). Thus, according to Definition 6, framework $(\mathcal{G}, p, \mathcal{A})$ is infinitesimal sign-elevation angle rigid. □

Theorem 4. *A framework $\mathcal{F}(\mathcal{G}, p, \mathcal{A})$ is sign-elevation angle rigid if it is infinitesimal sign-elevation angle rigid.*

Proof. The proof is similar to that of Theorem 2. □

1) Sign-elevation-Henneberg construction in 3-D: (Constructing globally sign-elevation angle rigid frameworks:) The following steps are followed to generate global sign elevation angle rigid frameworks in 3-D. For convenience, we adopt a similar nomenclature for it as for the 2-D case and denote this sign-elevation-Henneberg construction in 3-D. Here, new frameworks are generated by adding tetrahedral frameworks with one new signed-volume constraint. First, we assume the initial framework has $|\mathcal{V}| = 4, |\mathcal{E}| = 6$, and $\mathcal{A} = 1$. For a given globally sign elevation angle rigid framework $\mathcal{F}(\mathcal{G}, p, \mathcal{A})$, an

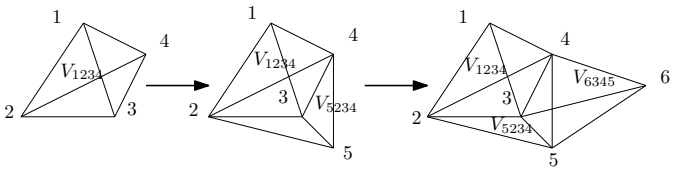


Fig. 5. Example of sign-elevation-Henneberg construction method for generating globally sign-elevation angle rigid frameworks in 3-D.

agent v is added to it such that it has three more elevation angle constraints and one signed-volume constraint. Now, the new framework $\bar{\mathcal{F}}(\bar{\mathcal{G}}, \bar{p}, \bar{\mathcal{A}})$ consists of tetrahedral frameworks and $\bar{\mathcal{G}} = (\bar{\mathcal{V}}, \bar{\mathcal{E}}), \bar{\mathcal{V}} = \mathcal{V} \cup \{v\}, \bar{\mathcal{E}} = \mathcal{E} \cup \{(i,v),(j,v),(k,v)\}, \bar{\mathcal{A}} = \mathcal{A} \cup \{(\bar{i},\bar{j},\bar{k},\bar{l})\}$, and $p = [p^\top \ p_v^\top]^\top \in \mathbb{R}^{3(n+1)}$, where $i,j,k \in \mathcal{V}$, with $(i,j),(j,k),(k,i) \in \mathcal{E}, \bar{i},\bar{j},\bar{k},\bar{l} \in \{i,j,k,v\}$ and $\bar{i} \neq \bar{j} \neq \bar{k} \neq \bar{l}$. Fig. 5 demonstrates these steps. It is important to note that here we cannot add the new edges to any arbitrary nodes $i,j,k \in \mathcal{V}$, but need to add the edges such that $(i,j),(j,k),(k,i) \in \mathcal{E}$ is satisfied, e.g., in Fig. 5 node 6 is added with edges to $3,4,5$; however, the addition of agent 6 to nodes $1,3,5$ is not allowed as $(1,5) \notin \mathcal{E}$. The reason behind such a construction will be clarified later.

Proposition 3. *An infinitesimally sign-elevation angle rigid framework $\mathcal{F}(\mathcal{G}, p, \mathcal{A})$ in 3-D is globally signed elevation angle rigid if it has sign-elevation-Henneberg construction.*

Proof. Proof is similar to that of Proposition 2. □

Definition 11. *(Strong Distance rigidity in 3-D) A distance rigid framework $\mathcal{F}(\mathcal{G}, p)$ in 3-D is called strongly distance rigid if we have $(p_i - p_j)$,$(p_i - p_k)$, and $(p_i - p_l)$ independent for all $(i,j),(i,k),(i,l) \in \mathcal{E}$.*

Proposition 4. *If a framework, $\mathcal{F}(\mathcal{G}, p)$, is strongly distance rigid in $\mathbb{R}^3$, then the signed framework $\mathcal{F}_1(\mathcal{G}_1, p, \mathcal{A})$ where $\mathcal{G}_1 = \mathcal{G}$, (i.e., sensing topology for distances in distance rigid graph $\mathcal{G}$ is same as elevation angle constraints in $\mathcal{G}_1$), is infinitesimally sign-elevation angle rigid in $\mathbb{R}^3$.*

Proof. Consider the signed framework $\mathcal{F}_1(\mathcal{G}_1, p, \mathcal{A})$ and replace its elevation angle constraints with distance constraints to obtain $\mathcal{G}$. As we have $\mathcal{F}(\mathcal{G}, p)$ strongly distance rigid in 3-D, using similar induction-based arguments in [10, Proposition 1], it can be proved that $\mathcal{F}(\mathcal{G}, p)$ is infinitesimal distance rigid. Now, a framework is elevation angle rigid if and only if it is distance rigid [35, Proposition 2]. Hence, the framework with elevation angle constraints $\mathcal{F}(\mathcal{G}_1, p)$ is elevation angle rigid. So, there exists a non zero $(3n-6) \times (3n-6)$ minor of R_e [35]. Now, from the definition of sign-elevation angle rigidity matrix $R_e^v = \begin{bmatrix} R_e \\ R_v \end{bmatrix}$ there exists a $3n-6 \times 3n-6$ non zero minor for R_e^v. Then, the proof follows from Theorem 3. □

D. Bearing-only formation control law using sign-elevation angle rigidity for n agents:

This section presents bearing-only control laws to achieve the desired formation specified by elevation angle and signed-area constraints considering n single integrators.

1) Control law for 2-D: We have the following elevation-angle constraints and the desired elevation-angle constraints specifying the formation in 2-D:

$$E(p) = [\dots, f_{ij}, \dots]^\top \in \mathbb{R}^{m_e}$$
$$E^* = [\dots, f_{ij}^*, \dots]^\top \in \mathbb{R}^{m_e},$$

where $f_{ij} = \cot(\alpha_{ij})$ and $f_{ij}^* = \cot^*(\alpha_{ij})$ for $(i,j) \in \mathcal{E}$. Also, we have the following signed-area and desired area constraints:

$$\bar{S} = \kappa[\dots, S_{ijk}, \dots]^\top \in \mathbb{R}^{m_s}$$
$$\bar{S}^* = \kappa[\dots, S_{ijk}^*, \dots]^\top \in \mathbb{R}^{m_s},$$

where $(i,j,k) \in \mathcal{A}$, and $\kappa > 0$ is a positive constant. The formation error is defined by

$$e(p) = [E^\top(p) \ \bar{S}^\top(p)]^\top - [E^{*\top} \ (\bar{S}^*)^\top]^\top. \tag{13}$$

Let $u = [u_1^\top, \dots, u_n^\top]^\top \in \mathbb{R}^{2n}$ contain the control inputs of all agents. The following gradient-based control law is proposed for single integrators:

$$\dot{p} = u = -h_c \nabla \Phi = -h_c \bar{R}_e^s(p)^\top e(p), \tag{14}$$

where $\Phi = \frac{1}{2} e^\top e$, and $\bar{R}_e^s = [R_e^\top \ \kappa R_s^\top]^\top$, which we call the modified sign-elevation angle rigidity matrix. Although κ is multiplied with the part corresponding to the signed area of the sign-elevation angle matrix, observe that Null$(\bar{R}_e^s)$ =Null(R_e^s) and Null$(\bar{R}_e^v)$ =Null(R_e^v), hence the rank of R_e^s is same as that of rank of $\bar{R}_e^s$. From (14), the control law for i-th agent is:

$$\dot{p}_i = u_i = -h_c (\bar{R}_e^s)^\top (i,:) e(p), \tag{15}$$

where $(\bar{R}_e^s)^\top(i,:)$ is the i-th row of $(\bar{R}_e^s)^\top$. Using (4) and (9), the i-th column of $\bar{R}_e^s$ is given by:

$$\begin{aligned} \bar{R}_e^s(:,i) = [0, \dots, -h_c^{-1} b_{ij}^\top, \dots, -h_c^{-1} b_{ik}^\top, 0, \dots, \\ - \kappa(h_c^{-1} f_{ij} b_{ij}^\top J + h_c^{-1} f_{ik} b_{ik}^\top J^\top), \dots, 0]^\top, \end{aligned} \tag{16}$$

where $(i,j),(i,k) \in \mathcal{E}$, and $(i,j,k) \in \mathcal{A}$. Here, $f_{ij} := \cot(\alpha_{ij}) = \frac{\cos(\alpha_{ij})}{\sin(\alpha_{ij})} = \frac{\bar{b}_{ij}^\top b_{ij'}}{\sqrt{1-(b_{ij}^\top b_{ij'})^2}}$. Hence, each term in $(\bar{R}_e^s(:,i))^\top$ only requires bearing measurements, i.e., b_{ij} and $b_{ij'}$. Also, the signed area constraints are $S_{ijk} = h_c^{-2} z_{ij}^\top J z_{ik} = f_{ij} f_{ik} b_{ij}^\top J b_{ik}$, and hence each term in F_e^s can also be calculated using bearing-only measurements. Therefore, the control law u_i requires bearing-only information. Also, from (16) and (14), it is clear that the control law (14) is free from h_c.

2) Control law for 3-D case: Similarly, we have the following signed volume and desired volume constraints for 3-D:

$$\bar{V} = \kappa[\dots, V_{ijkl}, \dots]^\top \in \mathbb{R}^{m_v}$$
$$\bar{V}^* = \kappa[\dots, V_{ijkl}^*, \dots]^\top \in \mathbb{R}^{m_v},$$

where $(i,j,k,l) \in \mathcal{A}$, and $\kappa > 0$ is a positive constant. The formation error is defined by

$$e(p) = [E(p)^\top \ \bar{V}^\top]^\top - [E^{*\top} \ (\bar{V}^*)^\top]^\top \tag{17}$$

Let $u = [u_1^\top, \ldots, u_n^\top]^\top$ contain the control inputs of all agents. The following gradient-based control law is proposed for the single integrators:

$$\dot{p} = u = -r_c \nabla \Phi = -r_c (\bar{R}_e^v(p))^\top e(p), \tag{18}$$

where $\Phi = \frac{1}{2} e^\top e$, and $\bar{R}_e^s = [R_e^\top \ \kappa R_v^\top]^\top$, which we call the modified sign-elevation angle rigidity matrices. Although κ is multiplied with the part corresponding to signed volume of the sign-elevation angle matrix, observe that Null$(\bar{R}_e^v)$ =Null(R_e^v), hence the rank of R_e^v is same as that of the of $\bar{R}_e^v$. From (18), the control law for i-th agent is:

$$\dot{p}_i = u_i = -r_c (\bar{R}_e^v)^\top (i,:)(F_e^v - (F_e^v)^*) \quad \text{for 3 D}, \tag{19}$$

where $(\bar{R}_e^v(:,i))^\top$ are the i-th row $(\bar{R}_e^v)^\top$. Using (4) and (12), the i-th column of $\bar{R}_e^v$ is given by:

$$\begin{aligned}\bar{R}_e^v(:,i) = [0, \ldots, -r_c^{-1} b_{ij}^\top, 0, \ldots, -r_c^{-1} b_{ik}^\top, 0 \ldots, -r_c^{-1} b_{il}^\top, \\ 0, \ldots, 0, -\kappa r_c^{-1} f_{ij} f_{ik} b_{ij}^\top [b_{ik}]^\times + \kappa r_c^{-1} f_{ij} f_{il} b_{ij}^\top [b_{il}]^\times + \\ \kappa r_c^{-1} f_{ik} f_{il} b_{il}^\top [b_{ik}]^\times, \ldots, 0]^\top,\end{aligned} \tag{20}$$

where $(i,j),(i,k),(i,l) \in \mathcal{E}$, $(i,j,k,l) \in \mathcal{A}$. Here, $f_{ij} := \text{cosec}(\frac{\alpha_{ij}}{2}) = \frac{1}{\sin(\frac{\alpha_{ij}}{2})} = \frac{1}{\sqrt{(1-\cos(\alpha_{ij}))/2}} = \frac{1}{\sqrt{(1-b_{ij'}^\top b_{ij''})/2}}$. Also, signed-volume constraints can be represented as $V_{ijkl} := r_c^{-3} z_{ij}^\top (z_{ik} \times z_{il}) = f_{ij} f_{ik} f_{il} b_{ij}^\top (b_{ik} \times b_{il})$. Hence, the control law u_i in 3-D also requires bearing-only information. Also, additional information on r_c is not required, which is clear from (18) and (20).

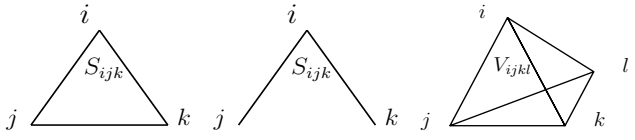
Remark 3. *Observe that for the control design, we have modified the signed-area and signed-volume constraints using a positive gain κ. The error function and the potential function are defined with these constraints. As discussed above, as the rank of the modified sign-elevation angle matrix ($\bar{R}_e^s$ or $\bar{R}_e^v$) is the same as R_e^s or R_e^v, introducing κ does not affect the rigidity properties of the frameworks. However, κ will play a crucial role in proving almost global stability with the gradient control laws* (14) *and* (18)*.*

Theorem 5. *Suppose $\mathcal{Q}$ denotes a set of p corresponding to formations of single integrators (described by* (1)*) that are congruent to a desired infinitesimal sign-elevation angle rigid formation. If the initial position $p(0) \in \mathcal{B}_{p^*}$, where $\mathcal{B}_{p^*}$ is a neighbourhood of p^*, and $p^* \in \mathcal{Q}$, using the control law* (14) *for 2-D or* (14) *for 3-D, $p(0)$ locally exponentially converges to a desired formation $p^{des} \in \mathcal{Q}$.*

Proof. This can be proved using the arguments of center manifold theorem [11], [39], [45], and hence is omitted. □

From Theorem 5, it is clear that under the control law (14) and (18), the desired configuration is a stable equilibrium point. However, it only establishes local convergence results. In the subsequent subsections, we establish almost global convergence for the frameworks generated by a sign-elevation-Henneberg construction with large κ, implying that for sufficiently large κ, we can not have other stable equilibriums.

Remark 4. *Observe that we have adopted a sign-elevation-Henneberg construction to construct a global sign-elevation angle rigid framework. However, we cannot conclude directly from this fact that under the control law* (14) *and* (18)*, we can achieve the desired configuration almost globally.*



(a) $\mathcal{F}_1(\mathcal{G}_1, \beta_1, \mathcal{A}_1)$ (b) $\mathcal{F}_l(\mathcal{G}_l, \beta_l, \mathcal{A}_l), l \in \{2, 3, \ldots, \psi\}$ (c) $\mathcal{F}_w(\mathcal{G}_w, \beta_w, \mathcal{A}_w), w \in \{1, 2, 3, \ldots, \psi\}$

Fig. 6. Examples of sub-frameworks $\mathcal{F}_l(\mathcal{G}_l, \beta_l, \mathcal{A}_l)$ for 2-D case for (a) $l = 1$, (b) $l \in \{1, 2, \ldots, \psi\}$, (c) Examples of sub-frameworks $\mathcal{F}_w(\mathcal{G}_w, \beta_w, \mathcal{A}_w)$ for 3-D case for $w \in \{1, 2, \ldots, \psi\}$

Now, we state the following Lemma, which will be helpful in our subsequent analysis.

Lemma 3. *Let $\beta_j (\in \mathbb{R}^6$ or $\in \mathbb{R}^{12}$ depending on 2-D or 3-D case, i.e., $d = 2$ or 3) be a regular point*[1] *for $F_{e_j}^s$ (or $F_{e_j}^v$) $j \in \{1, 2, \ldots, \psi\}$, then there exists a derivative map D_{ζ_i} of a map $\zeta_i(\beta_i)|_{\mathcal{G}_j}$ for β_i is in the neighborhood of β_j, i.e., $\beta_i \in \mathcal{B}_{\beta_j}$, close to $\mathcal{F}_j(\mathcal{G}_j, \beta_j, \mathcal{A}_j)$ such that*

$$D_{\zeta_i}(v_i)|_{\mathcal{G}_j} = \begin{cases} v_i \in \mathbb{R}^{d|\mathcal{V}_i|} \ \ \textit{if } i = j \\ v_i \in T_{\zeta_i(\beta_i)} F_{e_j}^{s\,-1} F_{e_j}^s(\beta_j) \ \textit{otherwise}, \end{cases}$$

where $T_x\mathcal{M}$ is the tangent space to a manifold $\mathcal{M}$ at point x.

Proof. The proof follows from [40, Lemma A1]. □

Remark 5. *From Lemma 1 (or 2) and Theorem 1 (or 3), we have β_j, $j \in \{1, 2, \ldots, \psi\}$ is a regular point of $F_{e_j}^s$(or $F_{e_j}^v$) implies the sub-frameworks are sign-elevation angle rigid. Hence, from Lemma 3 and [8, Proposition 2] $F_{e_j}^{s\,-1} F_{e_j}^s(\beta_j)$ (or $F_{e_j}^{v\,-1} F_{e_j}^v(\beta_j)$), $j \in \{1, 2, \ldots, \psi\}$ are the motions of $\mathcal{F}_j(\mathcal{G}_j, \beta_j, \mathcal{A}_j)$ in $SE(2)$(or $SE(3)$).*

E. Almost global stabilization for 2-D case

In this subsection, we establish almost global convergence result using the gradient control law (14) for 2-D case for sufficiently large κ with a sign-elevation-Henneberg construction.

As we have a sign-elevation-Henneberg construction, we split the framework $\mathcal{F}(\mathcal{G}, p, \mathcal{A})$ into ψ sub frameworks. Here, $\mathcal{F}(\mathcal{G}, p, \mathcal{A})$ is divided into $\mathcal{F}_l(\mathcal{G}_l, \beta_l, \mathcal{A}_l)$, $l \in \{1, 2, \ldots, \psi\}$. Each partition, $\mathcal{F}_l(\mathcal{G}_l, \beta_l, \mathcal{A}_l)$, consists of three agents, and hence for the sub-graph $\mathcal{G}_l = (\mathcal{V}_l, \mathcal{E}_l)$ we have $\mathcal{V}_l = \{i, j, k\}$ and $\beta_l = [p_i^\top \ p_j^\top \ p_k^\top]^\top \in \mathbb{R}^6$, $i, j, k \in \mathcal{V}_l$ is a realization associated with the sub-framework. Hence, $p = [\beta_1^\top \ \ldots \ \beta_\psi^\top]^\top \in \mathbb{R}^{2n}$. Further, we have $\mathcal{E} = \bigcup_{l=1}^{\psi} \mathcal{E}_l$ and $\mathcal{E}_l \cap \mathcal{E}_{l'} = \varnothing$, when $l, l' \in \{1, 2, \ldots, \psi\}, l \neq l'$, and $|\mathcal{E}_l| = 3$, for $l = 1$, and $|\mathcal{E}_l| = 2$ otherwise. Also, $\mathcal{A} = \bigcup_{l=1}^{\psi} \mathcal{A}_l$ with $\mathcal{A}_l \cap \mathcal{A}_{l'} = \varnothing$ when $l, l' \in \{1, 2, \ldots, \psi\}$ and $l \neq l'$ with $|\mathcal{A}_l| = 1$. It follows that $\mathcal{V} = \bigcup_{l=1}^{\psi} \mathcal{V}_l$ and $|\mathcal{V}_l| = 3$, and if β_l and $\beta_{l'}$ are adjacent for $l, l' \in \{1, 2, \ldots, \psi\}, l \neq l'$, then $\mathcal{V}_l \cap \mathcal{V}_{l'} \neq \varnothing$, else $\mathcal{V}_l \cap \mathcal{V}_{l'} = \varnothing$. This is illustrated in Fig. 6.

[1] [8] A realization β_j is a regular point of a function $F_{e_j}^s$ if rank$\left(\frac{\partial F_{e_j}^s}{\partial \beta_j}\right)$=max $\left\{\text{rank}\left(\frac{\partial F_{e_j}^s}{\partial \beta_j}\right) | \beta_j \in \mathbb{R}^{d|\mathcal{V}_j|}\right\}$

The following functions correspond to different sub-frameworks. The vectors contain the actual and the desired elevation angle constraints

$$E_l(\beta_l) = [\dots \ f_{ij} \ \dots]^\top \in \mathbb{R}^{|\mathcal{E}_l|} \tag{21}$$

$$E_l^*(\beta_l^*) = [\dots \ f_{ij}^* \ \dots]^\top \in \mathbb{R}^{|\mathcal{E}_l|}, \tag{22}$$

where $l \in \{1, 2, \dots, \psi\}$ and $(i, j) \in \mathcal{E}_l$. The actual and desired signed-area constraints for a sub-framework are

$$S_l(\beta_l) = \kappa S_{ijk} \in \mathbb{R}, \ S_l^* = \kappa S_{ijk}^* \in \mathbb{R}, \tag{23}$$

where $l \in \{1, 2, \dots, \psi\}$ and $(i, j, k) \in \mathcal{A}_l$. Hence, the formation error associated with each framework is

$$e_l(\beta_l) = [E_l^\top(\beta_l) \ S_l(\beta_l)]^\top - [E_l^{*\top} \ S_l^*]^\top := [e_{e_l}^\top \ e_{s_l}^\top]^\top, \tag{24}$$

where $e_{e_l} = E_l^\top - E_l^{*\top}, e_{s_l} = S_l - S_l^*$. The potential function for the sub-framework is given by $\Phi_l = \frac{1}{2}||e_l(\beta_l)||^2$, $l \in \{1, 2, \dots, \psi\}$ and the corresponding Hessian matrix is

$$\mathcal{H}_{\beta_l} = \frac{\partial^2 \Phi_l}{\partial \beta_l^2} \in \mathbb{R}^{6\times 6}, \tag{25}$$

while the sign-elevation angle rigidity matrix is

$$\bar{R}_{e_l}^s = \frac{\partial F_l}{\partial \beta_l} \in \mathbb{R}^{(|\mathcal{E}_l|+1)\times 6}, \ l \in \{1, 2, \dots, \psi\}, \tag{26}$$

with $F_l := [E_l^\top(\beta_l) \ S_l(\beta_l)]^\top \in \mathbb{R}^{|\mathcal{E}_l|+1}$ being the sign-elevation angle rigidity function associated with sub-framework $\mathcal{F}_l(\mathcal{G}_l, \beta_l, \mathcal{A}_l)$.

Lemma 4. *Consider a system of n single integrators with a framework $\mathcal{F}(\mathcal{G}, p, \mathcal{A})$, generated by a sign-elevation-Henneberg construction. If $p = p^*$ is a configuration corresponding to a stable equilibrium under the control law* (14)*, then for a sufficiently large $\kappa > 0$, the following statements hold*
(i) At equilibrium, the signed-area has the same sign as that of the desired area, i.e., sign of the equilibrium area must match the sign of the desired area.
(ii)At equilibrium, the framework $\mathcal{F}(\mathcal{G}, p^*, \mathcal{A})$, must be infinitesimally sign-elevation angle rigid.

Proof. The Hessian of Φ is also the negative Jacobian of the matrix in (14):

$$\mathcal{H}_p = \frac{\partial^2 \Phi}{\partial p^2} \in \mathbb{R}^{2n\times 2n}. \tag{27}$$

The Hessian associated with each sub-framework in given by:

$$\mathcal{H}_{\beta_l} = (R_{e_l}^s)^\top R_{e_l}^s + M_2 \otimes J + \bar{M}_1. \tag{28}$$

Let $p^\dagger$ be an equilibrium realization with an incorrect sign as that of the desired signed- area. This means that there exists a signed-area S_{ijk} such that at equilibrium, $S_{ijk} \leq 0$, while $S_{ijk}^* > 0, (i, j, k) \in \mathcal{A}$. So we may observe that for a sub-framework $\mathcal{F}_l(\mathcal{G}_l, \beta_l, \mathcal{A}_l), \ l \in \{1, 2, \dots, \psi\}$ we have $S_{ijk} - S_{ijk}^* \neq 0, (i, j, k) \in \mathcal{A}_l$ at $p^\dagger$. Now, we will show that when this happens, a negative eigenvalue for $\mathcal{H}_p$ at $p^\dagger$ results for sufficiently large κ, implying $p = p^\dagger$ is unstable for sufficiently large κ.

We will use a contradiction-based argument to prove this. First, assume that for sufficiently large κ, $p = p^\dagger$ is a stable equilibrium. As we have $\bar{R}_{e_l}^s = [R_{e_l}^\top \ \kappa R_{s_l}^\top]^\top$, where $R_{e_l} = \frac{\partial F_{e_l}^s}{\partial \beta_l}$ and $R_{s_l} = \frac{\partial S_{ijk}}{\partial \beta_l}$ for $(i, j, k) \in \mathcal{A}_l, l \in \{1, 2, \dots, \psi\}$, using (44) we may write

$$\mathcal{H}_{\beta_l} = R_{e_l}^\top R_{e_l} + \kappa^2 R_{s_l}^\top R_{s_l} + M_2 \otimes J + \bar{M}_1.$$

Next, we define a vector as $y := [y_1^\top \ \epsilon y_2^\top \ \mathbf{0}]^\top \in \mathbb{R}^6$, with $y_1 \in \mathbb{R}^2$ being unit vector perpendicular to $J^\top z_{jk}$ where $(i, j, k) \in \mathcal{A}_l$ and $l \in \{1, 2, \dots, \psi\}$, $y_2 \in \mathbb{R}^2$ is a non-zero vector with $\epsilon > 0$ being a small positive number. Hence, using the fact that $\frac{\partial S_{ijk}}{\partial \beta_l} = [z_{jk}^\top J \ z_{ik}^\top J \ z_{ij}^\top J], (i, j, k) \in \mathcal{A}_l, l \in \{1, 2, \dots, \psi\}$, we have

$$y^\top(\kappa^2 R_{s_l}^\top R_{s_l} + M_2 \otimes J)y \tag{29}$$

$$= \kappa^2 \underbrace{\epsilon^2 y_2^\top J^\top z_{ik} z_{ik}^\top J y_2}_{=y^\top R_{s_l}^\top R_{s_l} y} + \underbrace{\kappa\epsilon y_1^\top J y_2 e_{s_{ijk}}}_{=y^\top (M_2\otimes J)y}, \tag{30}$$

where $e_{s_{ijk}} = \kappa(S_{ijk} - S_{ijk}^*)$. Observe that (from Appendix (A)) the two terms $R_{e_l}^\top R_{e_l}$ and $\bar{M}_1$ are independent of κ. Thus for sufficiently large κ

$$y^\top \mathcal{H}_{\beta_l} y = \kappa^2(\epsilon y_1^\top J y_2(S_{ijk} - S_{ijk}^*) + O(\epsilon^2) + O(\bar{\epsilon^2})),$$

where $\bar{\epsilon} = \frac{1}{\kappa}$. Hence, we may choose y so that $y_1^\top J y_2(S_{ijk} - S_{ijk}^*)$ is negative and $y^\top \mathcal{H}_{\beta_l} y$ becomes negative definite at $p^\dagger$. Thus, for sufficiently large κ, when an incorrect sign for $(i, j, k) \in \mathcal{A}_l$ occurs, a negative eigenvalue exists for $\mathcal{H}_{\beta_l}$. Also, we have $\Phi = \sum_{l=1}^{\psi} \Phi_l$, which implies $\mathcal{H}_p = \sum_{l=1}^{\psi} \hat{\mathcal{H}}_{\beta_l}$, where $\hat{\mathcal{H}} = \frac{\partial^2 \Phi_l}{\partial p^2} \in \mathbb{R}^{2n\times 2n}$, and hence $\hat{\mathcal{H}}_{\beta_l}$ is constructed by adding zero rows and columns to $\mathcal{H}_{\beta_l}$. This implies that there exists $\hat{y} \in \mathbb{R}^{2n}$, which can be constructed by adding zeros to y such that $\hat{y}^\top \hat{\mathcal{H}}_{\beta_l} \hat{y} < 0$, and $\hat{\mathcal{H}}_{\beta_l}$ has at least one negative eigenvalue at $p^\dagger$.

Also, note that the sub-frameworks $\mathcal{F}_l(\mathcal{G}_l, \beta_l, \mathcal{A}_l), \ l \in \{1, 2, \dots, \psi\}$ has at least one agent common with the adjacent sub-framework $\mathcal{F}_l^{'}(\mathcal{G}_l^{'}, \beta_l^{'}, \mathcal{A}_l^{'}), \ l^{'} \in \{1, 2, \dots, \psi\} \backslash \{l\}$. Hence, $\mathcal{H}_p$ is not a block diagonal matrix consisting of $\mathcal{H}_{\beta_l}, l \in \{1, 2, \dots, \psi\}$ as the diagonal blocks. Hence, we cannot directly conclude that $\mathcal{H}_p$ has a negative eigenvalue at $p^\dagger$, from the fact that $\hat{\mathcal{H}}_{\beta_l}$ has a negative eigenvalue at $p^\dagger$. However, now we invoke Lemma 3 to reach this conclusion. From the above analysis, it is clear that with sufficiently large κ at equilibrium each of the sub-frameworks $\mathcal{F}_l(\mathcal{G}_l, \beta_l, \mathcal{A}_l), \ l \in \{1, 2, \dots, \psi\}$, which consists of three agents, are infinitesimally sign-elevation angle rigid configuration. Hence, from Lemma 1 and Theorem 1, $\bar{R}_{e_l}^s$ is of maximum row rank, which implies $\beta_l, l \in \{1, 2, \dots, \psi\}$ is a regular point for $F_{e_l}^s$. Also, we have span(L_p)$\subset$ Null($\hat{\mathcal{H}}_{\beta_l}$) [10, Lemma 2], [46] . Hence, it follows from Lemma 3 that there exists a vector $D_{\zeta_l}(\hat{y})|_{\mathcal{G}_l}$ such that

$$(D_{\zeta_l}(\hat{y})|_{\mathcal{G}_{l'}})^\top \hat{\mathcal{H}}_{\beta_l}(p^\dagger) D_{\zeta_l}(\hat{y})|_{\mathcal{G}_{l'}} = \begin{cases} \theta < 0 \text{ if } l = l' \\ 0 \text{ otherwise.} \end{cases} \tag{31}$$

Now, using the fact that $\mathcal{H} = \sum_{l=1}^{\psi} \hat{\mathcal{H}}_{\beta_l}$, we have $(D_{\zeta_l}(\hat{y})|_{\mathcal{G}_{l'}})^\top \mathcal{H}_p(p^\dagger) D_{\zeta_l}(\hat{y})|_{\mathcal{G}_{l'}} = \theta < 0$. Hence, we conclude for sufficiently large $\kappa > 0$, we can not have an incorrect

signed area at the equilibrium, i.e., we will have $S_{ijk} > 0$ if $S^*_{ijk} > 0$, and hence part (i) is proved. Further, note that this means we cannot have $S_{ijk} = 0$ at the equilibrium, which implies at equilibrium, the framework $\mathcal{F}(\mathcal{G}, p^\dagger, \mathcal{A})$ is strongly distance rigid. Using Proposition 1, we have the equilibrium framework as sign-elevation angle rigid, proving part (ii). □

We next present the following Theorem pertaining to the almost global convergence to a desired formation shape.

Theorem 6. *Consider a sign-elevation angle rigid framework constructed by sign-elevation-Henneberg construction in 2-D. Using control law* (14) *for single integrators as in* (1)*, there exists sufficiently large κ, such that the formation tracking error e almost globally converges to zero.*

Proof. We rewrite the control law in (14) as

$$\dot{p} = -(\bar{R}^s_e)^\top(p)e(p) = -R^\top_e(p)e_e(p) - \kappa R^\top_s(p)e_s(p) \quad (32)$$
$$= -R^\top_e(p)e_e(p) - \kappa^2 R^\top_s(p)e_s(p), \quad (33)$$

where $e_e(p) := E(p) - E^*, e_s(p) := \bar{S}(p) - \bar{S}^*, \bar{e}_s(p) := S(p) - S^*$. Now consider the Lyapunov candidate $\mathcal{L} := \frac{1}{2}e^\top e$, which is positive definite and radially unbounded. Taking its derivative along (14) yields

$$\dot{\mathcal{L}} = e^\top \dot{e} = -e^\top \bar{R}^s_e \bar{R}^{s\top}_e e = -||\bar{R}^{s\top}_e e||^2 \leq 0. \quad (34)$$

From, (34), we have $\dot{\mathcal{L}} \leq 0$. Hence, all the signals are bounded. Also, $\dot{\mathcal{L}} \equiv 0$, implies, $\bar{R}^{s\top}_e e \equiv 0$. Hence, the largest invariant set is given by the solution to $\bar{R}^{s\top}_e e \equiv 0$. Let, there exists non-zero $R^\top_e(p)e_e(p)$, and $R^\top_s(p)e_s(p)$ at equilibrium $p = p^*$ and $\bar{R}^{s\top}_e e = 0$, which implies from (32) that $-R^\top_e(p^*)e_e(p^*) - \kappa^2 R^\top_s(p^*)\bar{e}_s(p^*) = 0$. However, as e is bounded and hence R_e and R_s are also bounded, we may choose sufficiently large $\kappa > 0$ such that $-R^\top_e(p^*)e_e(p^*) - \kappa^2 R^\top_s(p^*)\bar{e}_s(p^*) \neq 0$, which is a contradiction. Hence, at equilibrium, we have

$$R^\top_e(p^*)e_e(p^*) = R^\top_s(p^*)\bar{e}_s(p^*) = 0. \quad (35)$$

From Lemma 4, we already know that for sufficiently large κ we have at equilibrium, the framework $(\mathcal{G}, p)$ being strongly distance rigid, implying $\text{rank}(R_e(p^*)) = 2n-3$. Hence, using the fact that we have a sign-elevation-Henneberg construction and $|\mathcal{E}| = 2n-3$, $R_e(p^*)$ is of full row rank. Therefore, we have $R^\top_e(p^*)e_e(p^*) = 0$, implying $e_e(p^*) = 0$. Also, from Lemma 4 for sufficiently large κ, note that the signed area at equilibrium has the same sign as that of the desired area. Now, as $e_e = 0$, implies the desired elevation angles, and hence, the desired distances are achieved, and the desired areas are also achieved, i.e., $e_s(p^*) = 0$. Hence, the largest invariant set is given by $e = 0$, hence using Lassal's invariance principle [47] we have e goes to zero asymptotically. □

Remark 6. *From Lemma 4 and Theorem 6, it is clear that there exists sufficiently large $\kappa > 0$ such that for a stable equilibrium p^* of the system* (14) *we will obtain the desired formation shape. However, system* (14) *may also have unstable equilibriums which is a set of measure zero and nowhere dense. Hence, the result of stability is almost global. Due to the nonlinear nature of gradient system* (14)*, finding these unstable equilibrium points is intractable.*

Remark 7. *Note that although the motivation for using a signed-area comes from [40], the control law in [40] is different than that of the proposed law here, and hence the structure of hessian in [40] is different here than in [40]. Also, [40] has used inter-agent displacements in the control law, whereas our control law uses bearing-only measurements. Also, in the next section, we will be proving stability for the 3-D case, whereas [40] was applicable for only planar graphs, i.e., 2-D agents.*

F. Almost global stabilization for 3-D

In this subsection, we establish almost global convergence in 3-D, using the gradient control law in (18) for sufficiently large values of κ with a sign-elevation-Henneberg construction for 3-D case.

As we have a sign-elevation-Henneberg construction, we may split the signed framework, $\mathcal{F}(\mathcal{G}, p, \mathcal{A})$, into ψ sub frameworks. Here, $\mathcal{F}(\mathcal{G}, p, \mathcal{A})$ is divided into $\mathcal{F}_w(\mathcal{G}_w, \beta_w, \mathcal{A}_w),\ w \in \{1, 2, \ldots, \psi\}$. Each partition, $\mathcal{F}_w(\mathcal{G}_w, \beta_w, \mathcal{A}_w)$, consists of four agents, and hence for the sub-graph $\mathcal{G}_w = (\mathcal{V}_w, \mathcal{E}_w)$ we have $\mathcal{V}_w = \{i, j, k, l\}$ and $\beta_w = [p_i^\top\ p_j^\top\ p_k^\top\ p_l^\top]^\top \in \mathbb{R}^{12},\ i, j, k, l \in \mathcal{V}_w$ is a realization associated with the sub-framework. Hence, $p = [\beta_1^\top\ \ldots\ \beta_\psi^\top]^\top \in \mathbb{R}^{3n}$. Also, we have $\mathcal{E} = \bigcup_{w=1}^{\psi} \mathcal{E}_w$ and $\mathcal{E}_w \cap \mathcal{E}_{w'} = \{(i, j), (j, k), (k, i)\}$, when $w, w^{'} \in \{1, 2, \ldots, \psi\}, w \neq w^{'}$, and $|\mathcal{E}_w| = 6$. Also, $\mathcal{A} = \bigcup_{w=1}^{\psi} \mathcal{A}_w$ with $\mathcal{A}_w \cap \mathcal{A}_{w'} = \varnothing$ when $w, w^{'} \in \{1, 2, \ldots, \psi\}$ and $w \neq w^{'}$ with $|\mathcal{A}_w| = 1$. It follows that $\mathcal{V} = \bigcup_{w=1}^{\psi} \mathcal{V}_w$ and $|\mathcal{V}_w| = 4$, and if β_w and $\beta_{w'}$ are adjacent for $w, w^{'} \in \{1, 2, \ldots, \psi\}, w \neq w^{'}$, then $\mathcal{V}_w \cap \mathcal{V}_{w'} \neq \varnothing$, otherwise $\mathcal{V}_w \cap \mathcal{V}_{w'} = \varnothing$. Examples of sub-frameworks are given in Fig. 6 (c). Observe that, unlike in 2-D, where there is no edges common for the sub-frameworks, for the 3-D case, there are always 3 edges that are common for any two adjacent sub-frameworks.

The following functions correspond to different sub-frameworks. The vectors contain the actual and the desired elevation angle constraints

$$E_w(\beta_w) = [\ldots\ f_{ij}\ \ldots]^\top \in \mathbb{R}^{|\mathcal{E}_w|} \quad (36)$$
$$E^*_w(\beta^*_w) = [\ldots\ f^*_{ij}\ \ldots]^\top \in \mathbb{R}^{|\mathcal{E}_w|}, \quad (37)$$

where $w \in \{1, 2, \ldots, \psi\}$ and $(i, j) \in \mathcal{E}_w$. The actual and desired signed-volume constraints for a sub-framework are

$$V_w(\beta_w) = \kappa V_{ijkl} \in \mathbb{R}, V^*_w = \kappa V^*_{ijkl} \in \mathbb{R}, \quad (38)$$

where $w \in \{1, 2, \ldots, \psi\}$ and $(i, j, k, l) \in \mathcal{A}_w$. The sign-elevation angle rigidity matrix is

$$\bar{R}^v_{e_w} = \frac{\partial F_w}{\partial \beta_w} \in \mathbb{R}^{(|\mathcal{E}_w|+1)\times 12},\ w \in \{1, 2, \ldots, \psi\}, \quad (39)$$

where $F_w := [E^\top_w(\beta_w)\ V_l(\beta_w)]^\top \in \mathbb{R}^{|\mathcal{E}_w|+1}$ is the sign-elevation angle rigidity function associated with a sub-framework, $\mathcal{F}_w(\mathcal{G}_w, \beta_w, \mathcal{A}_w)$. Hence, the formation error associated with each framework is

$$e_w(\beta_w) = [E^\top_w(\beta_w)\ V_w(\beta_w)]^\top - [E^{*\top}_w\ V^*_w]^\top. \quad (40)$$

Now, we modify the edge errors associated with the sub-frameworks such that the new error is divided by the number

of sub-frameworks connected with that edge, i.e., $\hat{e}_{e_{ij}} := \frac{1}{\sqrt{\varrho_{ij}}} e_{e_{ij}}$, where $e_{e_{ij}} := f_{ij} - f^*_{ij}$, and ϱ_{ij} is the number of sub-frameworks associated with edge (i,j). According to this definition, from Fig. 5, we have $\hat{e}_{e_{34}} := \frac{1}{\sqrt{3}} e_{e_{34}}$, i.e., $\varrho_{34} = 3$, and $\hat{e}_{e_{12}} := e_{e_{12}}$, i.e., $\varrho_{12} = 1$. Thus, we have the modified formation error associated with each sub-framework $w \in \{1, 2, \ldots, \psi\}$ given by

$$\hat{e}_w(\beta_w) = K e_w(\beta_w) \in \mathbb{R}^{|\mathcal{E}_w|+1}, \tag{41}$$

where $K = \text{Diag}\{\ldots, \frac{1}{\sqrt{\varrho_{ij}}} \ldots, 1\} \in \mathbb{R}^{(|\mathcal{E}_w|+1)\times(|\mathcal{E}_w|+1)}$, $(i,j) \in \mathcal{E}_w$. The potential function for the sub-framework is $\Phi_w = \frac{1}{2}||\hat{e}_w(\beta_w)||^2$, $w \in \{1, 2, \ldots, \psi\}$ and its Hessian is

$$\mathcal{H}_{\beta_w} = \frac{\partial^2 \Phi_w}{\partial \beta_w^2} \in \mathbb{R}^{12\times 12}. \tag{42}$$

Using this modified definition of edge errors, we have $\Phi = \sum_{w=1}^{\psi} \Phi_w$.

Lemma 5. *Consider a system of n single integrators and a framework $\mathcal{F}(\mathcal{G}, p, \mathcal{A})$, generated by a sign-elevation-Henneberg construction in 3-D. If $p = p^*$ is a configuration corresponding to a stable equilibrium under the control law* (18)*, then with sufficiently large $\kappa > 0$, the following hold:*
(i) At equilibrium, the signed volume has the same sign as the desired volume, i.e., the sign of the equilibrium volume must match with the sign of the desired volume.
(ii)At equilibrium, the frame work $\mathcal{F}(\mathcal{G}, p^*, \mathcal{A})$, must be infinitesimally sign-elevation angle rigid.

Proof. Let us calculate the Hessian of Φ, which is also the negative Jacobian matrix of (18):

$$\mathcal{H}_p = \frac{\partial^2 \Phi}{\partial p^2} \in \mathbb{R}^{3n\times 3n}. \tag{43}$$

The hessian associated with each sub-framework is given by:

$$\mathcal{H}_{\beta_l} = (R^v_{e_w})^\top K^4 R^v_{e_w} + \bar{N}_2 + \bar{N}_1. \tag{44}$$

Let $p^\dagger$ be a realization with an incorrect sign than that of the desired signed volume. This means there exists a signed-volume V_{ijkl} such that at equilibrium, $V_{ijkl} \leq$, while $V^*_{ijkl} > 0, (i,j,k,l) \in \mathcal{A}$. Observe that for a sub-framework $\mathcal{F}_w(\mathcal{G}_w, \beta_w, \mathcal{A}_w)$, $l \in \{1, 2, \ldots, \psi\}$ we will have $V_{ijkl} - V^*_{ijkl} \neq 0, (i,j,k,l) \in \mathcal{A}_w$ at $p^\dagger$. Now, we prove that when this happens, we have a negative eigenvalue for $\mathcal{H}_p$ at $p^\dagger$ for sufficiently large κ, making $p = p^\dagger$ an unstable equilibrium.

We use a contradiction-based argument. Assume that for sufficiently large κ, $p = p^\dagger$ is a stable equilibrium. As $\bar{R}^v_{e_w} = [R^\top_{e_w} \ \kappa R^\top_{v_w}]^\top$, where $R_{e_w} = \frac{\partial F_{e_w}}{\partial \beta_w}$ and $R_{v_w} = \frac{\partial V_{ijkl}}{\partial \beta_w}$ for $(i,j,k,l) \in \mathcal{A}_w, w \in \{1, 2, \ldots, \psi\}$, using (44) we may write

$$\mathcal{H}_{\beta_w} = R^\top_{e_w} \bar{K} R_{e_w} + \kappa^2 R^\top_{v_w} R_{v_w} + \bar{N}_1 + \bar{N}_2,$$

where $\bar{K} := \text{Diag}\{\ldots, \frac{1}{\varrho_{ij}{}^2}, \ldots\} \in \mathbb{R}^{|\mathcal{E}_w|\times|\mathcal{E}_w|}, (i,j) \in \mathcal{E}_w$. Define $y := [y_1^\top \ \epsilon y_2^\top \ \mathbf{0} \ \mathbf{0}]^\top \in \mathbb{R}^{12}$, with $y_1 \in \mathbb{R}^3$ being a unit vector perpendicular to $(z_{kl} \times z_{kj})$ where $(i,j,k,l) \in \mathcal{A}_w$ and $w \in \{1, 2, \ldots, \psi\}$, $y_2 \in \mathbb{R}^3$ is a non-zero vector with $\epsilon > 0$ being a small positive number. Using the fact that $\frac{\partial V_{ijk}}{\partial \beta_l} = r_c^{-3}[(z_{kl} \times z_{kj})^\top \ (z_{ik} \times z_{il})^\top \ (z_{il} \times z_{ij})^\top \ (z_{ij} \times z_{ik})^\top], (i,j,k,l) \in \mathcal{A}_w, w \in \{1, 2, \ldots, \psi\}$, we have

$$y^\top(\kappa^2 R^\top_{v_w} R_{v_w} + \bar{N}_2) y \tag{45}$$

$$= \kappa^2 \underbrace{\epsilon^2 y_2^\top (z_{ik} \times z_{il})(z_{ik} \times z_{il})^\top y_2}_{= y^\top R^\top_{v_w} R_{v_w} y} + \underbrace{\kappa \epsilon y_1^\top \Delta y_2 e_{v_{ijkl}}}_{= y^\top(\bar{N}_2) y}, \tag{46}$$

where $e_{v_{ijkl}} = \kappa(V_{ijkl} - V^*_{ijkl})$, and $\Delta := -[z_{kl}]^\times + [z_{ik}]^\times - [z_{il}]^\times = -2[z_{kl}]^\times \in \mathbb{R}^{3\times 3}$ (because $[z_{ik}]^\times - [z_{il}]^\times = -[z_{kl}]^\times$). Observe (from Appendix (B)) that these two terms $R^\top_{e_w} \bar{K} R_{e_w}$ and $\bar{N}_1$ are independent of κ, hence

$$y^\top \mathcal{H}_{\beta_w} y = \kappa^2(\epsilon y_1^\top \Delta y_2 (V_{ijkl} - V^*_{ijkl}) + O(\epsilon^2) + O(\bar{\epsilon^2})),$$

where $\bar{\epsilon} = \frac{1}{\kappa}$. We may thus can always choose y so that $y_1^\top \Delta y_2 (V_{ijkl} - V^*_{ijkl})$ is negative for sufficiently large κ. This is because due to our assumption $(V_{ijkl} - V^*_{ijkl}) > 0$ and $y_1^\top \Delta y_2 = \langle y_2, \Delta^\top y_1 \rangle$, we have to choose y_2 such that it makes an obtuse angle with the vector $\Delta^\top y_1$. Also, note that $\Delta^\top y_1 = 2[z_{kl}]^\times y_1 = 2(z_{kl} \times y_1)$, and hence, $\Delta^\top y_1$ is always a non-zero vector. Hence, $y^\top \mathcal{H}_{\beta_l} y$ is negative definite at $p^\dagger$. So, for sufficiently large κ, when an incorrect sign for $(i,j,k,l) \in \mathcal{A}_w$ occurs, $\mathcal{H}_{\beta_w}$ has a negative eigenvalue. We have $\Phi = \sum_{w=1}^{\psi} \Phi_w$, which implies $\mathcal{H}_p = \sum_{w=1}^{\psi} \hat{\mathcal{H}}_{\beta_w}$, where $\hat{\mathcal{H}} = \frac{\partial^2 \Phi_w}{\partial p^2} \in \mathbb{R}^{3n\times 3n}$. Hence $\hat{\mathcal{H}}_{\beta_w}$ is constructed by padding zero rows and columns to $\mathcal{H}_{\beta_w}$. This implies that there exists $\hat{y} \in \mathbb{R}^{3n}$, which can be constructed by adding zeros to y such that $\hat{y}^\top \hat{\mathcal{H}}_{\beta_w} \hat{y} < 0$, and $\hat{\mathcal{H}}_{\beta_w}$ has at least one negative eigenvalue at $p^\dagger$. Now, using Proposition 4 and Lemma 3 and using similar arguments as in the proof of Lemma 4, the proof follows. □

Theorem 7. *Consider a sign-elevation angle rigid framework constructed by a sign-elevation-Henneberg construction in 3-D. Using control law* (18) *for single integrator agents* (1)*, for sufficiently large κ, the formation tracking error e almost globally converges to zero.*

Proof. Proof follows similar lines as that of Theorem 6. □

G. Control design for non-holonomic agents

In this subsection, we propose control laws for non-holonomic agents, as described in equation (2), and demonstrate their stability using our proposed laws.

The following control laws are proposed

$$\begin{aligned} \bar{v}_i &= h_i^\top u_i \\ w_i &= h_i \times u_i \ i \in \mathcal{V}_i, \end{aligned} \tag{47}$$

where $u_i \in \mathbb{R}^d$ is the control input proposed for single integrators, i.e., the expression for u_i can be found in (14) for planar graphs (2-D) and (18) in 3-D.

Theorem 8. *Consider a sign-elevation angle rigid framework constructed by a sign-elevation-Henneberg construction in 2-D or 3-D. Using control law* (47) *for non-holonomic agents in* (2)*, with sufficiently large κ, the formation tracking error, e, almost globally converges to zero.*

Proof. Using the proposed control law in (47), the overall dynamics of n agents becomes

$$\dot{p} = H H^\top u, \quad \dot{h} = H^\perp (H^\perp)^\top u, \tag{48}$$

where $H := \text{diag}(h_1, \ldots, h_n) \in \mathbb{R}^{nd \times nd}, H^{\perp} := \text{diag}(h_1^{\perp}, \ldots, h_n^{\perp}) \in \mathbb{R}^{nd \times nd}$. Now, let the Lyapunov candidate be $\mathcal{L} = \frac{1}{2} e^{\top} e$, which is positive definite and radially unbounded. The time derivative of $\mathcal{L}$, along the system trajectory (48) is given by

$$\dot{\mathcal{L}} = e^{\top} \dot{e} = \begin{cases} e^{\top} \bar{R}_e^s \dot{p} = -e^{\top} \bar{R}_e^s H H^{\top} (\bar{R}_e^s)^{\top} e & \text{for } 2-D \\ e^{\top} \bar{R}_e^v \dot{p} = -e^{\top} \bar{R}_e^v H H^{\top} (\bar{R}_e^v)^{\top} e & \text{for } 3-D \end{cases}$$
$$= -||H^{\top} u||^2 \leq 0. \quad (49)$$

Form (49), it is clear that $\dot{\mathcal{L}}$ is negative semi-definite, and hence, all the signals are bounded. Now, when $\dot{\mathcal{L}} \equiv 0$, either (i) $u_i \equiv 0, \ \forall i \in \mathcal{V}$, or (ii) we have $h_i \perp u_i, u_i \not\equiv 0 \ \forall i \in \mathcal{V}$. Clearly, case (ii) cannot occur because if (ii) occurs, w_i would become non-zero and hence h_i will change and the condition in (ii) will not be satisfied. Hence, we have case (i) as the only possibility, and from Theorem 6 (and Theorem 7), it implies e approaches zero asymptotically. □

IV. ILLUSTRATIVE EXAMPLES

A. Single integrators in 2-D

Here, we first consider 6 single integrator agents (1) in 2-D. The desired configuration is generated by a sign-elevation-Henneberg construction in 2-D, with the edge set is $\mathcal{E} = \{(1,2),(2,3),(3,4),(4,1),(1,3),(5,3),(5,4),(6,1),(6,2)\}$ and the area index set is $\mathcal{A} = \{(4,3,1),(2,1,3),(5,3,4),(6,1,2)\}$. The desired formation shape is a hexagonal shape, with the desired elevation angle constraints $f_{12}^* = f_{34}^* = f_{53}^* = f_{54}^* = f_{61}^* = f_{62}^* = 10, f_{23}^* = f_{41}^* = 20, f_{13}^* = 10\sqrt{5}$, and the desired signed-area constraints $S_{431}^* = S_{213}^* = 200, S_{534}^* = S_{612}^* = 86.6$. The height of the rod is set as $h_c = 2$. The initial position of the agents are set to be $p_1(0) = [1.5 \ \ -9.1]^{\top}, p_2(0) = [5.4 \ \ -10.7]^{\top}, p_3(0) = [1.1, \ -14.7]^{\top}, p_4(0) = [-7.6 \ 15.5]^{\top}, p_5(0) = [8.9 \ 1.8]^{\top}$ and $p_6(0) = [15.7 \ 10.6]^{\top}$. First, we set $\kappa = 0$, i.e., no weights are given to the area constraints, and therefore, the control law becomes identical to the only elevation angle-based control laws proposed in [35]. Fig. 7 (a) shows the trajectories of the agents with $\kappa = 0$. The initial position of the agents are marked with circles and the final positions are marked with squares. The final formation shape is not the desired shape, since using only elevation angle constraints, the agents 5 and 6 have flipped from their desired positions. Hence, the final shape becomes ambiguous using the control law in [35]. Now, we set $\kappa = 0.02$ and Fig. 7 (b) shows the trajectories of the agents in this setup. Although agent 6 has gone to its desired position, still agent 5 has gone to the flipped position giving rise to an ambiguous shape. This is due to very low value of κ. Next, we increase κ to 0.1, and Fig. 7 (c) shows the trajectories of the agents. We may observe that now the desired formation shape is achieved.

B. Single integrators in 3-D

Next, we consider four agents in 3-D, with the edge set $\mathcal{E} = \{(1,2),(2,3),(3,1),(4,1),(4,2),(4,3),(5,1),(5,2),(5,3)\}$ and the volume index set $\mathcal{A} = \{(4,1,2,3),(5,1,2,3)\}$. The desired formation shape is a hexahedron with triangular faces, while the desired elevation angle constraints are given by $f_{ij}^* = 10, \ \forall (i,j) \in \mathcal{E}$, and the desired signed-volume constraints are $V_{4123}^* = -707.1068, V_{5123}^* = -707.1068$. The radius of the ball is $r_c = 0.1$. The initial positions of the agents are $p_1(0) = [1 \ -0.1 \ 0.1,]^{\top}, p_2(0) = [-1.2 \ 0.7 \ 0.9]^{\top}, p_3(0) = [1.1 \ 1.5 \ 1]^{\top}, p_4(0) = [0.8 \ 0.2 \ 2]^{\top}, p_5(0) = [0.6 \ 0.5 \ 1]^{\top}$. First we set $\kappa = 0$ and then the control law becomes identical with [35], and Fig. 8 (a) plots the trajectories of the agents in this case. We may observe that agents 4 and 5 are coinciding to one position giving rise to a final shape that is not congruent to the desired formation shape. Now, we set $\kappa = 0.02$ and the plot for this case is given in Fig. 8 (b), which indicates that the desired shape is achieved with our proposed law.

C. Non-holonomic agents

For non-holonomic agents, we consider the same desired formation shape as for the case of single integrators in 2-D, with the same desired elevation angle and signed-area constraints. The initial position of the agents are $p_1(0) = [-1.7 \ \ -4.1]^{\top}, p_2(0) = [1.2 \ 3.3]^{\top}, p_3(0) = [2.1 \ 5.1]^{\top}, p_4(0) = [-6.4 \ \ -7.4]^{\top}, p_5(0) = [11.6 \ 9.7,]^{\top}$ and $p_6(0) = [-3.1 \ 7.1]^{\top}$, and the initial headings of the agents are $h_1(0) = [1 \ 0]^{\top}, h_2(0) = [-1 \ 0]^{\top}, h_3(0) = [\frac{1}{\sqrt{2}} \ \frac{1}{\sqrt{2}}]^{\top}, h_4(0) = [0 \ 1]^{\top}, h_5(0) = [0 \ -1]^{\top}$ and $h_6(0) = [\frac{1}{\sqrt{3}} \ \frac{\sqrt{2}}{\sqrt{3}}]^{\top}$. The gain $\kappa = 0.1$, and Fig. 7 (d) shows the trajectories for the non-holonomic agents with our proposed control law (47), and the desired formation shape is achieved.

V. CONCLUSIONS

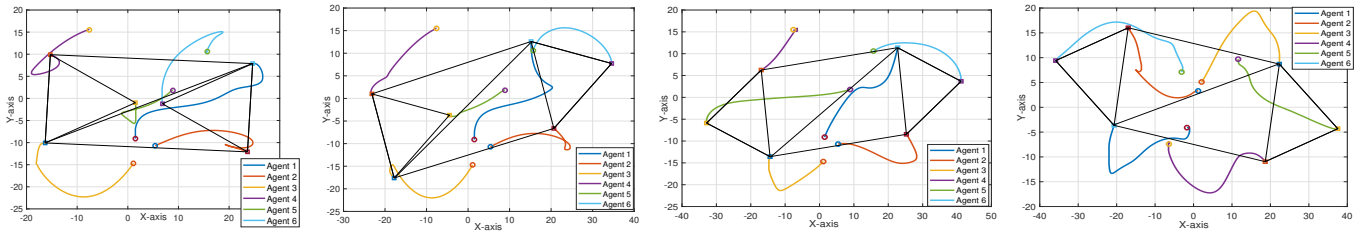
In this work, we have proposed sign-elevation angle rigidity for uniquely characterizing formation shapes using elevation angle and signed-area constraints or signed-volume constraints for 2-D and 3-D graphs, respectively. Then, bearing-only control laws are derived using only agents' local bearing information. Compared with the elevation angle rigidity-based control laws in [35], [37], which can only ensure local stability results, we have proved almost global results for the frameworks generated by sign-elevation-Henneberg construction, in which the overall framework consists of triangulated sub-frameworks for 2-D and tetrahedral sub-frameworks for 3-D. A gain parameter κ was introduced for signed-area and signed-volume constraints, and it was proved that there always exists sufficiently large κ such that agents can achieve the desired formation shape almost globally. Determining the exact lower bound for κ is a future topic for research. The results presented here can be extended for obtaining bearing-only formation maneuvers using similar maneuvering methods as in [35].

APPENDIX

(A) *Expression of Hessian for 2-D sub-frameworks:* The Hessian associated with the sub-framework for 2-D is

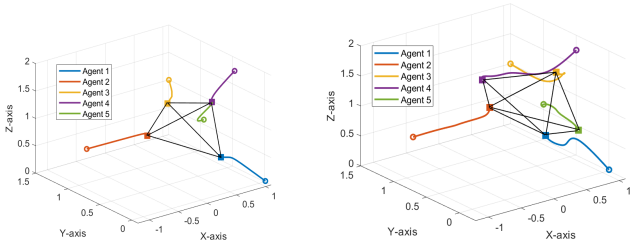
$$\mathcal{H}_{\beta_l} = \frac{\partial^2 \Phi_l}{\partial \beta_l^2} = \frac{\partial}{\partial \beta_l} (\bar{R}_{e_l}^{s \ \top} e_l) \in \mathbb{R}^{6 \times 6}, \quad (50)$$

where $e_l(\beta_l) = [E_l^{\top}(\beta_l) \ \ S_l(\beta_1)]^{\top} - [E_l^{* \top} \ \ S_l^*]^{\top}, \Phi_l = \frac{1}{2}||e_l(\beta_l)||^2$, and $\beta_l = [p_i^{\top} \ p_j^{\top} \ p_k^{\top}]^{\top}$. Consider $l = 1$, hence



(a) Single integrators with $\kappa = 0$ (b) Single integrators with $\kappa = 0.02$ (using [35]) (c) Single integrators with $\kappa = 0.1$ (d) Non-holonomic agents with $\kappa = 0.1$

Fig. 7. (a) Trajectories of single integrator agents with $\kappa = 0$, i.e., control law used is same as in [35], (b) Trajectories of single integrator agents with $\kappa = 0.02$, (c) Trajectories of single integrator agents with $\kappa = 0.1$, (d) Trajectories of non-holonomic agents with $\kappa = 0.1$.



(a) Trajectories of agents for $\kappa = 0$ (b) Trajectories of agents for $\kappa = 0.02$ (using [35])

Fig. 8. Trajectories of single integrators in 3-D for (a) $\kappa = 0$, (b) $\kappa = 0.02$.

$F_e^s = [f_{ij}\ f_{ik}\ f_{jk}\ \kappa S_{ijk}]^\top$ (Fig. 6(a)). The corresponding sign-elevation angle rigidity matrix is calculated as:

$$\bar{R}^s_{e_l} = \frac{\partial F^s_{e_l}}{\partial \beta_l} = h_c^{-1}\begin{bmatrix} -b_{ij}^\top & b_{ij}^\top & 0 \\ -b_{ik}^\top & 0 & b_{ik}^\top \\ 0 & -b_{jk}^\top & b_{jk}^\top \\ \kappa h_c^{-1} X^\top & -\kappa h_c^{-1} z_{ik}^\top J^\top & -\kappa h_c^{-1} z_{ij}^\top J \end{bmatrix},$$

where $X := (J^\top z_{ij} + J z_{ik})$, $F^s_{e_l} = [E_l^\top(\beta_l)\ S_l(\beta_l)]^\top \in \mathbb{R}^{|\mathcal{E}_l|+1}$. Hence, $(\bar{R}^s_{e_l})^\top e_l$ is calculated as

$$(\bar{R}^s_{e_l})^\top e_l = h_c^{-1}\begin{bmatrix} -e_{e_{ij}} b_{ij} - e_{e_{ik}} b_{ik} - h_c^{-1}\kappa X e_{s_{ijk}} \\ e_{e_{ij}} b_{ij} - e_{e_{jk}} b_{jk} + h_c^{-1}\kappa (J z_{ik}) e_{s_{ijk}} \\ e_{e_{ik}} b_{ik} - e_{e_{jk}} b_{jk} - h_c^{-1}\kappa (J^\top z_{ij}) e_{s_{ijk}} \end{bmatrix},$$

where $e_{e_{ij}} := f_{ij} - f^*_{ij}$ for $(i,j) \in \mathcal{E}_l$ and $e_{s_{ijk}} := \kappa(S_{ijk} - S^*_{ijk})$, for $(i,j,k) \in \mathcal{A}_l$. Now, the Hessian calculated as

$$\mathcal{H}_{\beta_l} = \frac{\partial}{\partial \beta_l}(\bar{R}^{s\ \top}_{e_l} e_l) \in \mathbb{R}^{6\times 6} = \bar{M}_1 + \bar{M}_2 + [C_{p_1}\ C_{p_2}\ C_{p_3}],$$

where

$$C_{p_1} = \begin{bmatrix} h_c^{-2} b_{ij} b_{ij}^\top + h_c^{-2} b_{ik} b_{ik}^\top + h_c^{-4}\kappa^2 X X^\top \\ -h_c^{-2} b_{ij} b_{ij}^\top - h_c^{-4}\kappa^2 J z_{ik} X^\top \\ -h_c^{-2} b_{ik} b_{ik}^\top - h_c^{-4}\kappa^2 J^\top z_{ij} X^\top \end{bmatrix}$$

$$C_{p_2} = \begin{bmatrix} -h_c^{-2} b_{ij} b_{ij}^\top - h_c^{-4}\kappa^2 (J^\top z_{ij} + J z_{ik})(J z_{ik})^\top \\ h_c^{-2} b_{ij} b_{ij}^\top + h_c^{-2} b_{jk} b_{jk}^\top + h_c^{-4}\kappa^2 (J z_{ik})(J z_{ik})^\top \\ -h_c^{-2} b_{jk} b_{jk}^\top + h_c^{-4}\kappa^2 (J^\top z_{ij})(J z_{ik})^\top \end{bmatrix}$$

$$C_{p_3} = \begin{bmatrix} -h_c^{-2} b_{ik} b_{ik}^\top - h_c^{-4}\kappa^2 (J^\top z_{ij} + J z_{ik})(J^\top z_{ij})^\top \\ -h_c^{-2} b_{jk} b_{jk}^\top + h_c^{-4}\kappa^2 (J z_{ik})(J^\top z_{ij})^\top \\ h_c^{-2} b_{ik} b_{ik}^\top + h_c^{-2} b_{jk} b_{jk}^\top + h_c^{-4}\kappa^2 (J^\top z_{ij})(J^\top z_{ij})^\top \end{bmatrix},$$

and $[C_{p_1}\ C_{p_2}\ C_{p_3}] = (\bar{R}^s_{e_l})^\top \bar{R}^s_{e_l}$ holds. Here, $\bar{M}_2 = M_2 \otimes I_2$,

$$M_2 = \begin{bmatrix} 0 & -h_c^{-2}\kappa e_{s_{ijk}} & h_c^{-2}\kappa e_{s_{ijk}} \\ h_c^{-2}\kappa e_{s_{ijk}} & 0 & h_c^{-2}\kappa e_{s_{ijk}} \\ -h_c^{-2}\kappa e_{s_{ijk}} & h_c^{-2}\kappa e_{s_{ijk}} & 0 \end{bmatrix} \text{ and}$$

$$\bar{M}_1 = h_c^{-1}\begin{bmatrix} Y_1 & -e_{e_{ij}}\frac{P_{b_{ij}}}{||z_{ij}||} & -e_{e_{ik}}\frac{P_{b_{ik}}}{||z_{ik}||} \\ -e_{e_{ij}}\frac{P_{b_{ij}}}{||z_{ij}||} & Y_2 & -e_{e_{jk}}\frac{P_{b_{jk}}}{||z_{jk}||} \\ -e_{e_{ik}}\frac{P_{b_{ik}}}{||z_{ik}||} & -e_{e_{jk}}\frac{P_{b_{jk}}}{||z_{jk}||} & Y_3 \end{bmatrix}$$

where $Y_1 = e_{e_{ij}}\frac{P_{b_{ij}}}{||z_{ij}||} + e_{e_{ik}}\frac{P_{b_{ik}}}{||z_{ik}||}$, $Y_2 = e_{e_{ij}}\frac{P_{b_{ij}}}{||z_{ij}||} + e_{e_{jk}}\frac{P_{b_{jk}}}{||z_{jk}||}$, and $Y_3 = e_{e_{ik}}\frac{P_{b_{ik}}}{||z_{ik}||} + e_{e_{jk}}\frac{P_{b_{jk}}}{||z_{jk}||}$, with $P_{b_{ij}}$ is the projection matrix defined by $P_{b_{ij}} := I_2 - b_{ij} b_{ij}^\top$.

For $l \in \{2, \ldots, \psi\}$, we have $F^s_e = [f_{ij}\ f_{ik}\ S_{ijk}]^\top$ (Fig. 6(b)). Hence the sign elevation angle rigidity matrix (R^s_e) for these sub-frameworks can be obtained by deleting row 4 from the expression of R^s_e calculated for $l = 1$. For calculating the Hessian for this case, expression for $\bar{M}_2$ remains the same as that of calculated for $w = 1$, and $\bar{M}_1$ becomes

$$\bar{M}_1 = h_c^{-1}\begin{bmatrix} Y_1 & -e_{e_{ij}}\frac{P_{b_{ij}}}{||z_{ij}||} & -e_{e_{ik}}\frac{P_{b_{ik}}}{||z_{ik}||} \\ -e_{e_{ij}}\frac{P_{b_{ij}}}{||z_{ij}||} & e_{e_{ij}}\frac{P_{b_{ij}}}{||z_{ij}||} & 0 \\ -e_{e_{ik}}\frac{P_{b_{ik}}}{||z_{ik}||} & 0 & e_{e_{ik}}\frac{P_{b_{ik}}}{||z_{ik}||} \end{bmatrix} \quad (51)$$

where $Y_1 = e_{e_{ij}}\frac{P_{b_{ij}}}{||z_{ij}||} + e_{e_{ik}}\frac{P_{b_{ik}}}{||z_{ik}||}$.

(B) *Expression of Hessian for 3-D sub-frameworks :* Now, we calculate the Hessian associated with the sub-framework in the case of 3-D, which is given by

$$\mathcal{H}_{\beta_w} = \frac{\partial^2 \Phi_w}{\partial \beta_w^2} = \frac{\partial}{\partial \beta_w}(\bar{R}^{v\ \top}_{e_w} K^2 e_w) \in \mathbb{R}^{12\times 12}, \quad (52)$$

where $e_w(\beta_w) = [E_w^\top(\beta_w)\ S_w(\beta_w)]^\top - [E_w^{*\top}\ S_w^*]^\top$, $\Phi_w = \frac{1}{2}||\hat{e}_w(\beta_w)||^2$, and $\beta_w = [p_i^\top\ p_j^\top\ p_k^\top\ p_l^\top]^\top$. Consider $w \in \{1, \ldots, \psi\}$, hence $F^v_e = [f_{ij}\ f_{ik}\ f_{il}\ f_{kj}\ f_{kl}\ f_{jl}\ \kappa V_{ijkl}]^\top$ (Fig. 6(c)). The sign-elevation angle rigidity matrix is calculated as:

$$\bar{R}^v_{e_w} = \frac{\partial F^v_{e_w}}{\partial \beta_w} = \frac{1}{r_c}\begin{bmatrix} -b_{ij}^\top & b_{ij}^\top & 0 & 0 \\ -b_{ik}^\top & 0 & b_{ik}^\top & 0 \\ -b_{il}^\top & 0 & 0 & b_{il}^\top \\ 0 & b_{kj}^\top & -b_{kj} & 0 \\ 0 & 0 & -b_{kl}^\top & b_{kl}^\top \\ 0 & -b_{jl}^\top & 0 & b_{jl}^\top \\ r_c^{-2}\kappa Z_1^\top & r_c^{-2}\kappa Z_2^\top & r_c^{-2}\kappa Z_3^\top & r_c^{-2}\kappa Z_4^\top \end{bmatrix},$$

where $Z_1 = z_{kl} \times z_{kj}, Z_2 = z_{ik} \times z_{il}, Z_3 = z_{il} \times z_{ij}, Z_4 = z_{ij} \times z_{ik}$. Note that $Z_1 = -Z_2 - Z_3 - Z_4$. Now, the Hessian is calculated as

$$\mathcal{H}_{\beta_w} = \frac{\partial}{\partial \beta_w}(\bar{R}^v_{e_w}{}^\top K^2 e_w) = \bar{N}_1 + \bar{N}_2 + (\bar{R}^v_{e_w})^\top K^4 \bar{R}^v_{e_w},$$

where $\bar{N}_2 = \frac{\kappa e_{v_{ijkl}}}{r_c^3} N_2 \in \mathbb{R}^{12\times 12}$, and $N_2 =$

$$\begin{bmatrix} 0 & -[z_{kl}]^\times & [z_{kl}]^\times - [z_{kj}]^\times & [z_{kj}]^\times \\ [z_{ik}]^\times - [z_{il}]^\times & 0 & [z_{il}]^\times & -[z_{ik}]^\times \\ [z_{il}]^\times - [z_{ij}]^\times & -[z_{kl}]^\times & 0 & [z_{ij}]^\times \\ [z_{ij}]^\times - [z_{ik}]^\times & [z_{ik}]^\times & -[z_{ij}]^\times & 0 \end{bmatrix}$$

and $\bar{N}_1 =$

$$r_c^{-1} \begin{bmatrix} Y_1 & -\frac{P_{b_{ij}}}{||z_{ij}||}\tilde{e}_{e_{ij}} & -\frac{P_{b_{ik}}}{||z_{ik}||}\tilde{e}_{e_{ik}} & -\frac{P_{b_{il}}}{||z_{il}||}\tilde{e}_{e_{il}} \\ -\frac{P_{b_{ij}}}{||z_{ij}||}\tilde{e}_{e_{ij}} & Y_2 & -\frac{P_{b_{kj}}}{||z_{kj}||}\tilde{e}_{e_{kj}} & -\frac{P_{b_{jl}}}{||z_{jl}||}\tilde{e}_{e_{jl}} \\ -\frac{P_{b_{ik}}}{||z_{ik}||}\tilde{e}_{e_{ik}} & -\frac{P_{b_{kj}}}{||z_{kj}||}\tilde{e}_{e_{kj}} & Y_3 & -\frac{P_{b_{kl}}}{||z_{kl}||}\tilde{e}_{e_{kl}} \\ -\frac{P_{b_{il}}}{||z_{il}||}\tilde{e}_{e_{il}} & -\frac{P_{b_{jl}}}{||z_{jl}||}\tilde{e}_{e_{jl}} & -\frac{P_{b_{kl}}}{||z_{kl}||}\tilde{e}_{e_{kl}} & Y_4 \end{bmatrix},$$

where $Y_1 = \frac{P_{b_{ij}}}{||z_{ij}||}\tilde{e}_{e_{ij}} + \frac{P_{b_{ik}}}{||z_{ik}||}\tilde{e}_{e_{ik}} + \frac{P_{b_{il}}}{||z_{il}||}\tilde{e}_{e_{il}}, Y_2 = \frac{P_{b_{ij}}}{||z_{ij}||}\tilde{e}_{e_{ij}} + \frac{P_{b_{kj}}}{||z_{kj}||}\tilde{e}_{e_{kj}} + \frac{P_{b_{jl}}}{||z_{jl}||}\tilde{e}_{e_{jl}}, Y_3 = \frac{P_{b_{ik}}}{||z_{ik}||}\tilde{e}_{e_{ik}} + \frac{P_{b_{kj}}}{||z_{kj}||}\tilde{e}_{e_{kj}} + \frac{P_{b_{kl}}}{||z_{kl}||}\tilde{e}_{e_{kl}}, Y_4 = \frac{P_{b_{il}}}{||z_{il}||}\tilde{e}_{e_{il}} + \frac{P_{b_{jl}}}{||z_{jl}||}\tilde{e}_{e_{jl}} + \frac{P_{b_{kl}}}{||z_{kl}||}\tilde{e}_{e_{kl}}$, with $P_{b_{ij}} := I_3 - b_{ij}b_{ij}^\top \in \mathbb{R}^{3\times 3}$ is the projection matrix, and $\tilde{e}_{e_{ij}} := \frac{1}{\varrho_{ij}} e_{e_{ij}}, (i,j) \in \mathcal{E}_w$.

REFERENCES

[1] B. D. Anderson, C. Yu, B. Fidan, and J. M. Hendrickx, "Rigid graph control architectures for autonomous formations," *IEEE Control Systems Magazine*, vol. 28, no. 6, pp. 48–63, 2008.

[2] G.-Z. Yang, J. Bellingham, P. E. Dupont, P. Fischer, L. Floridi, R. Full, N. Jacobstein, V. Kumar, M. McNutt, R. Merrifield *et al.*, "The grand challenges of science robotics," *Science robotics*, vol. 3, no. 14, p. eaar7650, 2018.

[3] Z. Sun, S. Mou, B. D. Anderson, and M. Cao, "Exponential stability for formation control systems with generalized controllers: A unified approach," *Systems & Control Letters*, vol. 93, pp. 50–57, 2016.

[4] S. Zhao and D. Zelazo, "Bearing rigidity and almost global bearing-only formation stabilization," *IEEE Transactions on Automatic Control*, vol. 61, no. 5, pp. 1255–1268, 2015.

[5] S. Coogan and M. Arcak, "Scaling the size of a formation using relative position feedback," *Automatica*, vol. 48, no. 10, pp. 2677–2685, 2012.

[6] J. A. Fax and R. M. Murray, "Information flow and cooperative control of vehicle formations," *IFAC Proceedings Volumes*, vol. 35, no. 1, pp. 115–120, 2002.

[7] W. Ren and E. Atkins, "Distributed multi-vehicle coordinated control via local information exchange," *International Journal of Robust and Nonlinear Control: IFAC-Affiliated Journal*, vol. 17, no. 10-11, pp. 1002–1033, 2007.

[8] L. Asimow and B. Roth, "The rigidity of graphs, ii," *Journal of Mathematical Analysis and Applications*, vol. 68, no. 1, pp. 171–190, 1979.

[9] J. Cortés, "Global and robust formation-shape stabilization of relative sensing networks," *Automatica*, vol. 45, no. 12, pp. 2754–2762, 2009.

[10] X. Chen, M.-A. Belabbas, and T. Başar, "Global stabilization of triangulated formations," *SIAM Journal on Control and Optimization*, vol. 55, no. 1, pp. 172–199, 2017.

[11] T. H. Summers, C. Yu, S. Dasgupta, and B. D. Anderson, "Control of minimally persistent leader-remote-follower and coleader formations in the plane," *IEEE Transactions on Automatic Control*, vol. 56, no. 12, pp. 2778–2792, 2011.

[12] G. Jing, G. Zhang, H. W. Joseph Lee, and L. Wang, "Weak rigidity theory and its application to formation stabilization," *SIAM Journal on Control and optimization*, vol. 56, no. 3, pp. 2248–2273, 2018.

[13] S.-H. Kwon and H.-S. Ahn, "Generalized rigidity and stability analysis on formation control systems with multiple agents," in *2019 18th European Control Conference (ECC)*. IEEE, 2019, pp. 3952–3957.

[14] A. N. Bishop, M. Deghat, B. D. Anderson, and Y. Hong, "Distributed formation control with relaxed motion requirements," *International Journal of Robust and Nonlinear Control*, vol. 25, no. 17, pp. 3210–3230, 2015.

[15] S. Zhao and D. Zelazo, "Localizability and distributed protocols for bearing-based network localization in arbitrary dimensions," *Automatica*, vol. 69, pp. 334–341, 2016.

[16] ——, "Translational and scaling formation maneuver control via a bearing-based approach," *IEEE Transactions on Control of Network Systems*, vol. 4, no. 3, pp. 429–438, 2015.

[17] K. Cao, D. Li, and L. Xie, "Bearing-ratio-of-distance rigidity theory with application to directly similar formation control," *Automatica*, vol. 109, p. 108540, 2019.

[18] S. Zhao and D. Zelazo, "Bearing rigidity theory and its applications for control and estimation of network systems: Life beyond distance rigidity," *IEEE Control Systems Magazine*, vol. 39, no. 2, pp. 66–83, 2019.

[19] S. Zhao, Z. Li, and Z. Ding, "Bearing-only formation tracking control of multiagent systems," *IEEE Transactions on Automatic Control*, vol. 64, no. 11, pp. 4541–4554, 2019.

[20] Z. Tang, R. Cunha, T. Hamel, and C. Silvestre, "Formation control of a leader–follower structure in three dimensional space using bearing measurements," *Automatica*, vol. 128, p. 109567, 2021.

[21] ——, "Relaxed bearing rigidity and bearing formation control under persistence of excitation," *Automatica*, vol. 141, p. 110289, 2022.

[22] J. Zhao, X. Yu, X. Li, and H. Wang, "Bearing-only formation tracking control of multi-agent systems with local reference frames and constant-velocity leaders," *IEEE Control Systems Letters*, vol. 5, no. 1, pp. 1–6, 2020.

[23] C. Garanayak and D. Mukherjee, "Distributed fixed-time orientation synchronization with application to formation control," in *2021 60th IEEE Conference on Decision and Control (CDC)*. IEEE, 2021, pp. 7130–7135.

[24] Q. Van Tran, M. H. Trinh, D. Zelazo, D. Mukherjee, and H.-S. Ahn, "Finite-time bearing-only formation control via distributed global orientation estimation," *IEEE Transactions on Control of Network Systems*, vol. 6, no. 2, pp. 702–712, 2018.

[25] C. Garanayak and D. Mukherjee, "Formation control in agents' local coordinate frames for arbitrary initial attitudes," *IEEE Transactions on Control of Network Systems*, pp. 1–12, 2024.

[26] Q. Van Tran, H.-S. Ahn, and B. D. Anderson, "Distributed orientation localization of multi-agent systems in 3-dimensional space with direction-only measurements," in *2018 IEEE Conference on Decision and Control (CDC)*. IEEE, 2018, pp. 2883–2889.

[27] G. Michieletto, A. Cenedese, and A. Franchi, "Bearing rigidity theory in se (3)," in *2016 IEEE 55th Conference on Decision and Control (CDC)*. IEEE, 2016, pp. 5950–5955.

[28] D. Zelazo, P. R. Giordano, and A. Franchi, "Bearing-only formation control using an se (2) rigidity theory," in *2015 54th ieee conference on decision and control (cdc)*. IEEE, 2015, pp. 6121–6126.

[29] L. Chen, M. Cao, and C. Li, "Angle rigidity and its usage to stabilize multi-agent formations in 2d," *IEEE Transactions on Automatic Control*, 2020.

[30] L. Chen and M. Cao, "Angle rigidity for multi-agent formations in 3d," *IEEE Transactions on Automatic Control*, 2023.

[31] G. Jing, G. Zhang, H. W. J. Lee, and L. Wang, "Angle-based shape determination theory of planar graphs with application to formation stabilization," *Automatica*, vol. 105, pp. 117–129, 2019.

[32] L. Chen, "Triangular angle rigidity for distributed localization in 2d," *Automatica*, vol. 143, p. 110414, 2022.

[33] L. Chen and Z. Sun, "Globally stabilizing triangularly angle rigid formations," *IEEE Transactions on Automatic Control*, vol. 68, no. 2, pp. 1169–1175, 2022.

[34] N. P. K. Chan, B. Jayawardhana, and H. G. de Marina, "Angle-constrained formation control for circular mobile robots," *IEEE Control Systems Letters*, vol. 5, no. 1, pp. 109–114, 2021.

[35] L. Chen and Z. Sun, "Gradient-based bearing-only formation control: An elevation angle approach," *Automatica*, vol. 141, p. 110310, 2022.

[36] C. Garanayak and D. Mukherjee, "Bearing-only formation control for double integrators and non-holonomic agents with elevation-angle rigidity," in *2023 9th International Conference on Control, Decision and Information Technologies (CoDIT)*. IEEE, 2023, pp. 736–741.

[37] ——, "Bearing-only formation control with bounded disturbances in agents' local coordinate frames," *IEEE Control Systems Letters*, 2023.

[38] B. D. Anderson, Z. Sun, T. Sugie, S.-i. Azuma, and K. Sakurama, "Formation shape control with distance and area constraints," *IFAC Journal of Systems and Control*, vol. 1, pp. 2–12, 2017.

[39] S.-H. Kwon, Z. Sun, B. Anderson, and H.-S. Ahn, "Hybrid distance-angle rigidity theory with signed constraints and its applications to formation shape control," *arXiv preprint arXiv:1912.12952*, 2019.
[40] S.-H. Kwon, Z. Sun, B. D. Anderson, and H.-S. Ahn, "Sign rigidity theory and application to formation specification control," *Automatica*, vol. 141, p. 110291, 2022.
[41] K. Li, Z. Shen, G. Jing, and Y. Song, "Angle-constrained formation control under directed non-triangulated sensing graphs," *Automatica*, vol. 163, p. 111565, 2024.
[42] L. Chen, L. Xie, X. Li, X. Fang, and M. Feroskhan, "Simultaneous localization and formation using angle-only measurements in 2d," *Automatica*, vol. 146, p. 110605, 2022.
[43] C. Garanayak and D. Mukherjee, "Bearing-only formation control using sign-elevation angle rigidity for avoiding formation ambiguities." in *2023 American Control Conference*. IEEE, 2023, pp. 2684–2689.
[44] C. Godsil and G. F. Royle, *Algebraic graph theory*. Springer Science & Business Media, 2001, vol. 207.
[45] S. Wiggins, S. Wiggins, and M. Golubitsky, *Introduction to applied nonlinear dynamical systems and chaos*. Springer, 2003, vol. 2, no. 3.
[46] M. Field, "Equivariant dynamical systems," *Transactions of the American Mathematical Society*, vol. 259, no. 1, pp. 185–205, 1980.
[47] H. K. Khalil, "Nonlinear systems(3rd edn)," 2002.



Chinmay Garanayak is a doctoral student at the Department of Electrical Engineering, Indian Institute of Technology Bombay. He received his B.Tech. (2015) from the National Institute of Technology, Rourkela, India, in Electrical Engineering. His research interests include autonomous systems, formation control, and vision-based control of networked systems.



Dwaipayan Mukherjee is an Assistant Professor of Electrical Engineering at Indian Institute of Technology Bombay. He received his B. E. (2007) from Jadavpur University, Kolkata, in Electrical Engineering and M.Tech. (2009) in Control Systems Engineering from the Indian Institute of Technology Kharagpur. In 2014, he completed his Ph.D. from the Indian Institute of Science, Bangalore, Dept. of Aerospace Engineering. From 2015-2017 he was a post-doctoral fellow at the Faculty of Aerospace Engineering, Technion− Israel Institute of Technology. His research interests include multi-agent systems, co-operative control, and control theory.